CHAPTER-2(A)

Metal(II) chloride complexes containing a tridentate N-donor Schiff base ligand: syntheses, structures and antimicrobial activity.

Abstract

One new tridentate N-coordinate ligand N′-Phenyl-N″-(phenyl(pyridin-2-yl)methylene)ethane-1,2-diamine (L1) has been synthesized and characterized. The tridentate N_3-coordinate ligand L1 has been used in the synthesis of a series of three mononuclear complexes $[M(L1)Cl_2]$ [M = Cu(II), Co(II), and Zn(II)] and one polynuclear Cd(II) complex $[Cd(L1)Cl_2]_n$ and these complexes were characterized by spectroscopic techniques. The structure of all the complexes have been solved by single crystal X-ray diffraction studies and the data reveals that all mononuclear complexes have distorted square pyramidal geometry and polynuclear Cd(II) complex have distorted octahedral geometry. The antimicrobial activity of all complexes were investigated against Gram positive (*Bacillus subtilis, Staphylococcus aureus*) and Gram negative (*Escherichia coli, Proteus vulgaris*) bacteria by disk diffusion method. All the compounds demonstrated significant antimicrobial activity while $[Cd(L1)Cl_2]_n$ exhibited the best antibacterial activity among all the synthesized complexes.

2(A).1. Introduction

The coordination chemistry of transition metal complexes using Schiff base ligands have been an interesting area of research in inorganic chemistry. This is because of the fact that the transition metal complexes with Schiff bases have wide applications in many scientific areas such as biological activities, polymer, pharmacy etc [1-5]. The Schiff bases have been used as versatile chelating ligands because they form stable complexes with most of the transition metal ions and they have significant importance in coordination chemistry. The transition metal ions are most important for this as they can adopt different oxidation states and geometries. Schiff base ligands with more than two coordination sites are of particular interest as they not only form stable complexes but also form complexes with different geometries due to the presence of different donating atoms which are important for the catalytic and magnetic properties of the complexes. There are many reports on the transition metal complexes with Schiff base ligands using more than two donor atoms [6-27]. As our interest is to study the coordination properties and biological activities of transition metal complexes using Schiff base ligands, we have synthesized one new tridentate N_3-donor Schiff base ligand and its multinuclear complexes.

In the present work, we report on the synthesis and characterization with structure of N_3-donor Schiff base ligand N′-Phenyl-N′′-(phenyl(pyridin-2-yl)methylene)ethane-1,2-diamine (L1) and its mononuclear complexes [M(L1)Cl_2] [M = Cu(II), Co(II) and Zn(II)] and polymeric complex [Cd(L1)Cl_2]$_{n.}$ The complexes were investigated for their antimicrobial potential.

2(A).2. Experimental

2(A).2.1. Materials

The chemicals and solvents were analytical grade and purchased from commercial sources. N-phenylethene-1,2-diamine, 2-benzoylpyridine (Aldrich), $CuCl_2.2H_2O$ (Loba, India), $CoCl_2.6H_2O$, $ZnCl_{2.}$ and $CdCl_2$ (Sisco chem, India) were reagent grade and used as received.

2(A).2.2. Synthesis of Ligand (L1)

Synthesis of N′-Phenyl-N′′-(phenyl(pyridin-2-yl)methylene)ethane-1,2-diamine(L1)

To the solution of N-phenylethene-1,2-diamine (1.361 g, 10 mmol) in ethanol (30 mL), a solution of 2-benzoyl pyridine (1.832 g, 10 mmol) in the same solvent (15 mL) was added dropwise with stirring. The reaction mixture was then refluxed for 8 h. The solution was concentrated on a vacuum rotary evaporator and the light-yellow coloured solid product was isolated by filtration and recrystallized in hot ethanol.

Yield. 2.55g (80%). Found C = 79.51, H = 6.23, N = 13.57%, Elemental analysis calc. for $C_{20}H_{19}N_3$: C = 79.65, H = 6.30, N = 13.94 %. IR (KBr, pellet, cm^{-1}): ν(N-H), 3295 s; ν(C=N), 1605 s; ν (C=C)+ ν (C=N)py, 1582 w; ν (C=C)ph, 1534 w. ^1H NMR (400 MHz, $CDCl_3$, 20°C δ ppm); 3.45 (s, 2H, N-CH_2-CH_2 of ethylene), 3.66 (d, 2H, J = 8Hz, N-CH_2-CH_2 of ethylene), 6.72 (s, 1H, Ph/ring), 6.65(d, 2H, J = 8 Hz, Ph/ring), 7.23 – 7.58 (m, 7H, Ph/ring), 7.60(s, 1H, Py/ring), 7.61(s, 1H, Py/ring), 7.77(s, 1H, Py/ring), 8.64 (s, 1H, N-CH Py/ring).

2(A).2.3. Syntheses of Complexes

2(A).2.3.1. [Cu(L1)Cl_2] (1)

To a stirring methanol solution (10 mL) of $CuCl_2.2H_2O$ (0.042 g, 0.25 mmol), the Schiff base ligand L1 (0.075 g, 0.25 mmol) in methanol (10 mL) was added drop by drop and the colour changed immediately from light green to dark green. This mixture was stirred for 3 h at room temperature, filtered and green coloured crystals were obtained after slow evaporation of the solvent.

Yield. 0.087 g (80%). Found C = 55.36, H = 4.22, N = 9.46%. Elemental analysis calc. for $C_{20}H_{19}N_3Cl_2Cu$: C = 55.06, H = 4.35, N = 9.63%. IR (KBr, pellet, cm^{-1}): ν(N-H), 3380s; ν(C=N), 1633s; ν(C=C)+ ν(C=N)Py, 1597m; ν(C=C)Ph, 1492m; ν(M-N), 463w. λ_{max}/nm (ε_{max} /mol^{-1} cm^{-1}). 628(312), 399(2326), 302(6439). Λ_M ($\Omega^{-1}cm^2\,mol^{-1}$) = 10. μ_{eff} = 1.80 BM.

2(A).2.3.2. [Co(L1)Cl_2] (2)

The complex was prepared by following the same method as that of complex **1** except $CoCl_2$ salt was added instead of $CuCl_2$ salt. Dark Purple coloured crystals were obtained after slow evaporation of the solution.

Yield. 0.080 g (72%). Found C = 55.66, H = 4.15, N = 9.63%. Elemental analysis calc. for $C_{20}H_{19}N_3Cl_2Co$: C = 55.65, H = 4.40, N = 9.74%. IR (KBr, pellet, cm^{-1}): ν(N-H), 3223s; ν(C=N), 1633s; (C=C)+ ν(C=N)py, 1594w; ν(C=C)Ph, 1492w; ν(M-N), 453w. λ_{max}/nm (ε_{max}/mol^{-1} cm^{-1}). 796(72), 507(105), 350 (8177), 271(8787). Λ_M ($\Omega^{-1}cm^2\,mol^{-1}$) = 15. μ_{eff} = 3.87 BM.

2(A).2.3.3. [Zn(L1)Cl_2] (3)

The complex was prepared by following the same method as that of Cu (II) complex except $ZnCl_2$ salt was added instead of $CuCl_2$ salt. Light yellow coloured crystals were obtained after slow evaporation of the solution.

Yield. 0.085 g (78%). Found C = 54.87, H = 4.25, N = 9.52%. Elemental analysis calc. for $C_{20}H_{19}N_3Cl_2Zn$: C = 54.83, H = 4.34, N = 9.59 %. IR (KBr, pellet, cm^{-1}): ν (N-H), 3233s; ν(C=N), 1633m; ν(C=C)+ υ(C=N)py, 1597m; ν(C=C)Ph, 1494 m; ν(M-N), 453w. λ_{max}/nm (ε_{max} /mol^{-1} cm^{-1}). 360(1205), 274(4429), 219(5192). Λ_M ($\Omega^{-1}cm^2\,mol^{-1}$) = 12.

2(A).2.3.4. [Cd(L1)Cl_2]$_n$ (4)

The complex was prepared by following the same method as that of complex **1** except $CdCl_2$ salt was added instead of $CuCl_2$ salt. Colorless crystals were obtained after slow evaporation of the solution.

Yield. 0.082 g (68%). Found C =49.36, H = 3.86, N = 8.75%. Elemental analysis calc. for $C_{20}H_{19}N_3Cl_2Cd$: C = 49.51, H = 3.92, N = 8.66%. IR (KBr, pellet, cm^{-1}): ν (N-H) 3373 s; ν(C=N), 1630 s; ν(C=C)+ ν(C=N)py, 1597 m; ν(C=C)Ph, 1498m; ν(M-N), 438w. λ_{max}/nm (ε_{max} /mol^{-1} cm^{-1}). 399(1036), 354(2767), 278 (11668), 234 (15192). Λ_M ($\Omega^{-1}cm^2\,mol^{-1}$) = 15.

2(A).2.4. Physical Measurements

The FT-IR spectrum were recorded on a Bruker Alpha spectrometer using KBr pellets. The micro analyses (C, H and N) were carried out using a Thermo finnigan Flash EA 1112 series elemental analyzer. UV-Vis spectra (850 - 190 nm) of the ligand and complexes were recorded on a JASCO V630 in CH_3CN solution (1 x 10^{-3} M). X-band EPR measurements were performed on a JES-FA200 EPR spectrometer in liquid nitrogen temperature (77 K). Solution conductivity were measured in acetonitrile solution using Equip-Tronics conductivity meter (model no. EQ660 A). Room temperature magnetic susceptibilities of powder samples were measured using Guoy balance.

2(A).2.5. Antimicrobial activity assay

The antimicrobial activity of the compounds was tested against Gram positive (*Bacillus subtilis, Streptococcus aureus*) and Gram negative (*Escherichia Coli, Proteus Vulgaris*) bacteria by using disk diffusion method. Various concentrations of the ligand and the complexes were prepared in DMSO. The overnight grown bacterial cultures were spread on 4 mm thick Luria Bertani (LB) agar plates. DMSO and chloramphenicol at various concentration were used as a negative control and positive control, respectively. Then Whatman filter paper disks of 5 mm impregnated in the test samples or the controls were placed on the LB agar surface. The assay was performed in duplicates. The plates were then incubated at 37°C for 24 h. The plates were checked for appearance of zones of inhibition after incubation. The lowest concentration of the test sample which prevented visible growth of microorganism, which thus resulted in the formation of zone was considered as MIC of that sample.

2(A).3. X-ray Crystallography

The X-ray single crystal data of ligand and compounds **1**, **2**, **3** and **4** were collected on Oxford X-CALIBUR-S diffractometer equipped with CCD detector. The details of crystallographic data collection and some important features of the structure refinements of the complexes are given in Table 2(A).1. Data were collected with Mo-Kα radiation (λ= 0.71073 Å) at 293 K for all the compounds. The data interpretations were processed with CrysAlisPro, Agilent Technologies, Version 1.171.35.19 [28]. Absorption corrections were applied based on multi-scan method [29]. The structures were solved by direct methods and refined by the full-matrix least-square method based on F^2 technique using SHELXL-97 program package [30]. All calculations were carried out using WinGX system Ver-1.64 crystallographic software [31]. All non-hydrogen atoms were refined anisotropically. The positions of the hydrogen atoms were calculated from the difference Fourier map, placed in the calculated positions and constrained to ride on their parent atoms. ORTEP3 windows program were used for generating for molecular graphics [32].

2(A).4. Results and discussion

2(A).4.1. Syntheses

The Schiff base ligand N′-Phenyl-N′′-(phenyl(pyridin-2-yl)methylene)ethane-1,2-diamine (L1) was synthesized as a light-yellow solid by the condensation of 2-benzoylpyridine and N-Phenyl-ethylenediamine in ethanol [Scheme 2(A).1]. The ligand was characterized by ^{1}H NMR, FT-IR and structure determination by single crystal X-ray diffraction studies [Fig. 2(A).10]. The ligand is tridentate with N_3- coordination sites. The mononuclear complexes $[M(L1)Cl_2]$ [M = Cu(II), Co(II) and Zn(II)] and the polymeric complex $[Cd(L1)Cl_2]_n$ were obtained with good yield (>65%) upon one-pot synthesis of 1:1 mole ratio of metal chloride salts and tridentate Schiff base ligand L1 in ethanol at room temperature [Scheme 2(A).2]and

Table 2(A).1. Crystallographic data for ligand and Complexes.

	Ligand (L1)	**[Cu(L1)Cl_2]**	**[Co(L1)Cl_2]**	**[Zn(L1)Cl_2]**	**[Cd(L1)Cl_2]$_n$**
Empirical formula	$C_{20}H_{19}N_3$	$C_{20}H_{19}N_3Cl_2Cu$	$C_{20}H_{19}N_3Cl_2Co$	$C_{20}H_{19}N_3Cl_2Zn$	$C_{20}H_{19}N_3Cl_2Cd$
Formula weight	301.39	435.82	431.21	437.65	484.68
Temperature(K)	293(2)	293(2)	293(2)	293(2)	293(2)
Crystal system	Monoclinic	Monoclinic	Monoclinic	Monoclinic	Triclinic
Space group	$P2_1/c$	$P2_1/n$	$P2_1/n$	$P2_1/n$	P-1
a(Å)	11.0684(16)	7.6731(5)	7.8332(6)	7.8332(6)	6.9712(10)
b(Å)	7.4680(10)	16.6429(10)	16.6979(11)	16.6979(11)	9.9514(8)
c(Å)	20.378(3)	14.8484(9)	14.9982(10)	14.9982(10)	15.3955(16)
α(°)	90	90	90	90	92.713(7)
β(°)	105.284(14)	95.746(6)	94.228(6)	94.228(6)	92.760(10)
γ(°)	90	90	90	90	106.968(10)
Volume($Å^3$)	1624.9(4)	1886.7(2)	1956.4(2)	1956.4(2)	1018.3(2)
Z	4	4	4	4	2
ρ_{calc}(g/cm^3)	1.2320	1.534	1.464	1.486	1.581
μ(mm^{-1})	0.074	1.449	1.159	1.537	1.343
F(000)	640.2	892.0	884.0	896.0	484.0
Crystal size(mm^3)	0.6 × 0.4 × 0.2	0.3 × 0.2 × 0.2	0.3 × 0.2 × 0.2	0.3 × 0.2 × 0.2	0.3 × 0.2 × 0.2
Radiation(Å)	Mo Kα (λ = 0.71073)	Mo Kα (λ = 0.71073)	Mo Kα (λ = 0.71073)	Mo Kα (λ = 0.71073)	MoKα (λ = 0.71073)
2Θ range for data collection(°)	6.66 to 58.38	6.03 to 58.49	6.53 to 58.31	6.53 to 58.31	6.124 to 58.506
Index ranges	$-15 \le h \le 13, -10 \le k \le 9, -27 \le l \le 27$	$-10 \le h \le 10, -22 \le k \le 21, -20 \le l \le 19$	$-10 \le h \le 10, -22 \le k \le 21, -20 \le l \le 19$	$-10 \le h \le 10, -22 \le k \le 21, -20 \le l \le 19$	$-9 \le h \le 9, -13 \le k \le 13, -20 \le l \le 20$
Reflections collected	9839	21399	21699	21699	21254

Independent reflections	3769 [R_{int} = 0.0343, R_{sigma} = 0.0505]	4549 [R_{int} = 0.0873, R_{sigma} = 0.0878]	4692 [R_{int} = 0.0671, R_{sigma} = 0.0641]	4692 [R_{int} = 0.0671, R_{sigma} = 0.0641]	4865 [R_{int} = 0.1332, R_{sigma} = 0.1277]
Data/restraints/parameters	3769/0/208	4549/0/239	4692/0/239	4692/0/239	4865/0/235
Goodness-of-fit on F^2	1.052	1.051	1.046	0.991	0.999
Final R indexes [I≥2σ (I)]	R_1 = 0.0532, wR_2 = 0.1090	R_1 = 0.0612, wR_2 = 0.0884	R_1 = 0.0565, wR_2 = 0.1220	R_1 = 0.0485, wR_2 = 0.0792	R_1 = 0.0663, wR_2 = 0.1512
Final R indexes [all data]	R_1 = 0.1035, wR_2 = 0.1362	R_1 = 0.1058, wR_2 = 0.1007	R_1 = 0.0934, wR_2 = 0.1406	R_1 = 0.0847, wR_2 = 0.0922	R_1 = 0.1353, wR_2 = 0.1950
Largest diff. peak/hole (eÅ^{-3})	0.36/-0.28	0.43/-0.41	0.62/-0.56	0.31/-0.31	1.54/-1.10
CCDC	1960451	1982792	2044943	1982791	1982790

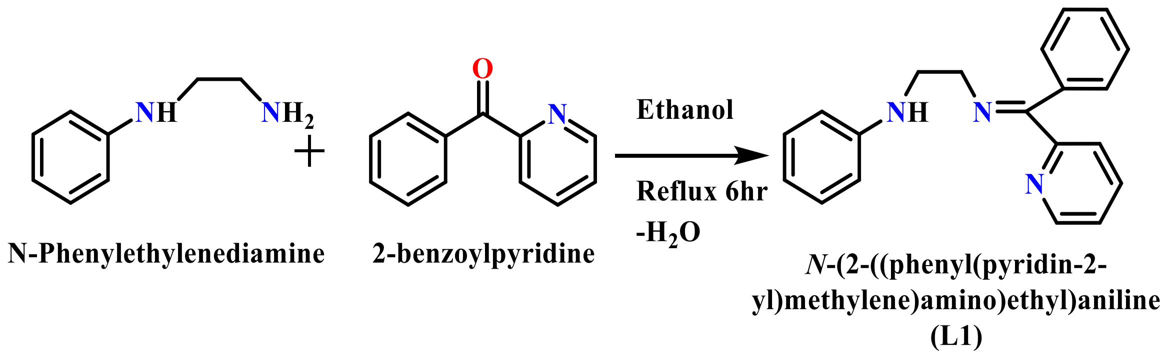

Scheme 2(A).1. Synthesis of ligand (L1)

characterized by elemental analysis, UV-Vis, FT-IR and single crystal X-ray diffraction studies. The ligand L1 is tridentate and has utilized it's all three nitrogen donor atoms for coordination with metal ions in the mononuclear complexes but in case of polymeric cadmium(II) complex, the tridentate ligand L1 has utilized only two nitrogen donor atoms for coordination. The coordination of ligand L1 in the metal centres were confirmed by FT-IR and single crystal X-ray diffraction studies. Mononuclear complexes are five coordinated with distorted square pyramidal geometry but the polynuclear Cd(II) complex has six coordination and the geometry around Cd centre is distorted octahedral. Molar conductivity measurements in CH_3CN shows all the complexes are non-electrolyte and there was no change in conductivity even after 3h indicating no dissociation of the complexes in solution. The compounds are soluble in all common organic solvents like acetonitrile, methanol, ethanol, acetone, dichloromethane etc.

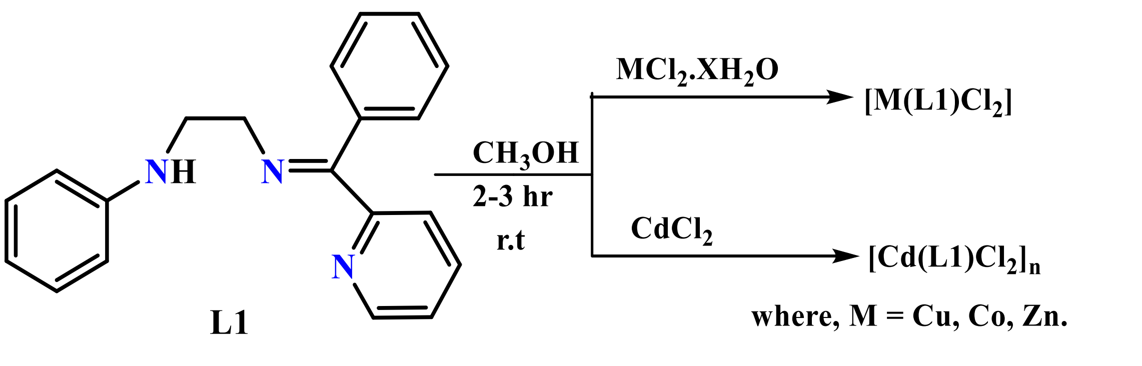

Where, X = 6 for Co(II) and 2 for Cu(II)

Scheme 2(A).2. Syntheses of complexes

2(A).4.2. Spectral Data

2(A).4.2.1. ^{1}H NMR spectral Data

The ^{1}H NMR spectrum of ligand L1 shows one singlet and one doublet appeared in the region at 3.45 and 3.66 ppm confirms the presence of –CH_2–CH_2– group of ethylenediamine moiety. The aromatic protons of phenyl ring appear at 6.65 -7.77 ppm as multiplet. One singlet appeared in the region at 8.64 ppm confirms the presence of proton of pyridine ring.

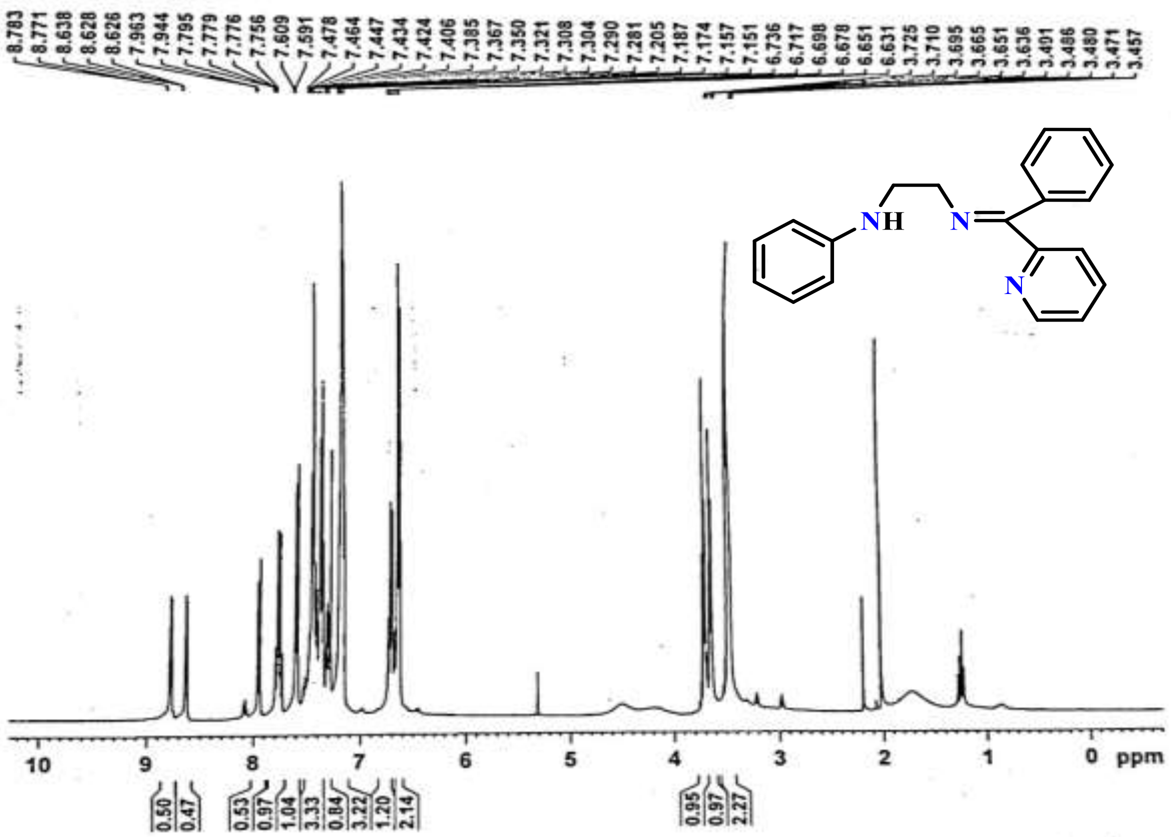

Figure. 2(A).1. ^{1}H NMR spectrum of Ligand (L1)

2(A).4.2.2. Mass spectral data

Mass spectrum of the synthesized Schiff base ligand (L1) confirmed the proposed formula by detecting the following peaks. The observed peak at m/z 301 ($C_{30}H_{30}N_3$), represents the molecular ion peak of the Schiff base with 100% abundance. The other molecular ion peaks (m/z 77, 106 and 195) appeared in the mass spectra are attributed to the fragmentation of molecule obtained from the rupture of different bonds inside the molecule. From the data we concluded that the molecular weight was in good agreement with the calculated molecular weight of the investigated ligand L1.

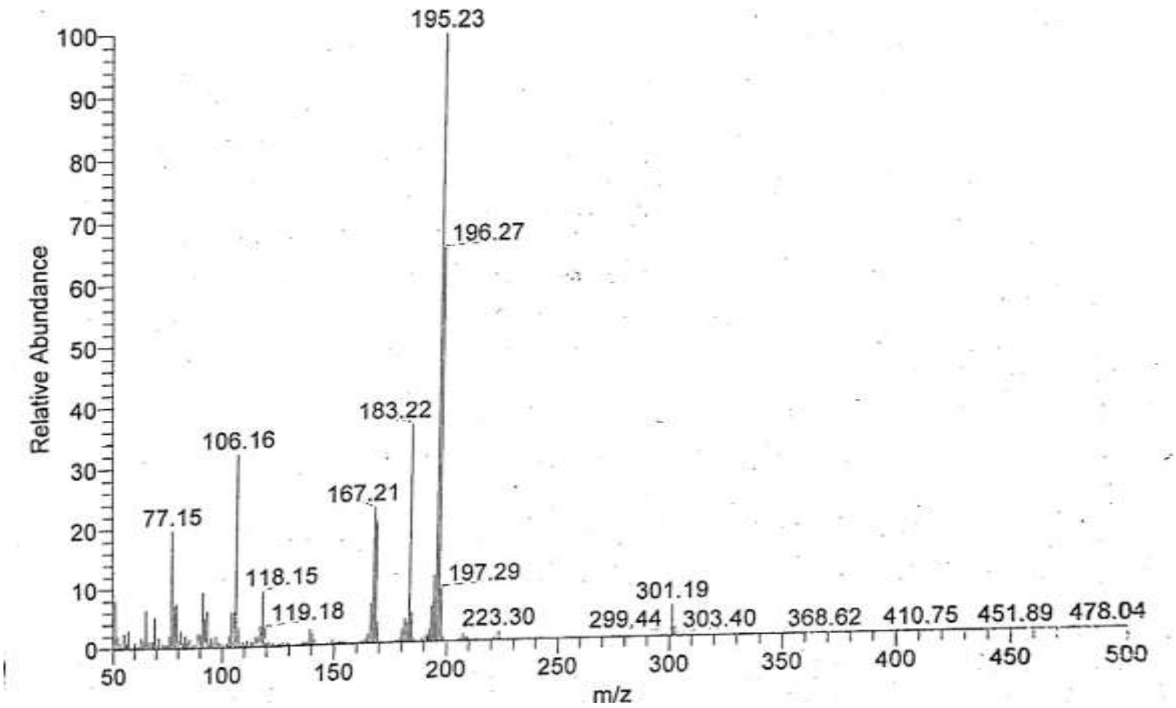

Figure. 2(A).2. Mass spectrum of Ligand (L1)

2(A).4.2.3. IR spectral data

IR spectrum of ligand exhibited several strong bands. Among these one strong band exhibited at 3295 cm^{-1} due to ν(N-H), one sharp band at 1605 cm^{-1} due to ν(C=N), one strong band at 1582 cm^{-1} due to ν(C=C)+ ν(C=N) of the pyridine ring and at 1534 cm^{-1} due to ν(C=C) of the benzene ring [15]

The IR spectrum of the complexes were assigned in comparison to the spectrum of the Schiff base ligand L1. In all the complexes, one sharp band exhibited at ~3213 cm^{-1} due to ν(NH) and another strong absorption bands exhibited at ~1641 cm^{-1} due to ν(C=N) group. These two absorption bands are also present in the ligand but shifted to lower wave numbers which may be attributed to the coordination of the ligand with the metal centres. The IR spectrum of Cd (II) complex exhibited a broad band at 3211 cm^{-1} due to free ν(N–H) vibrations [33].

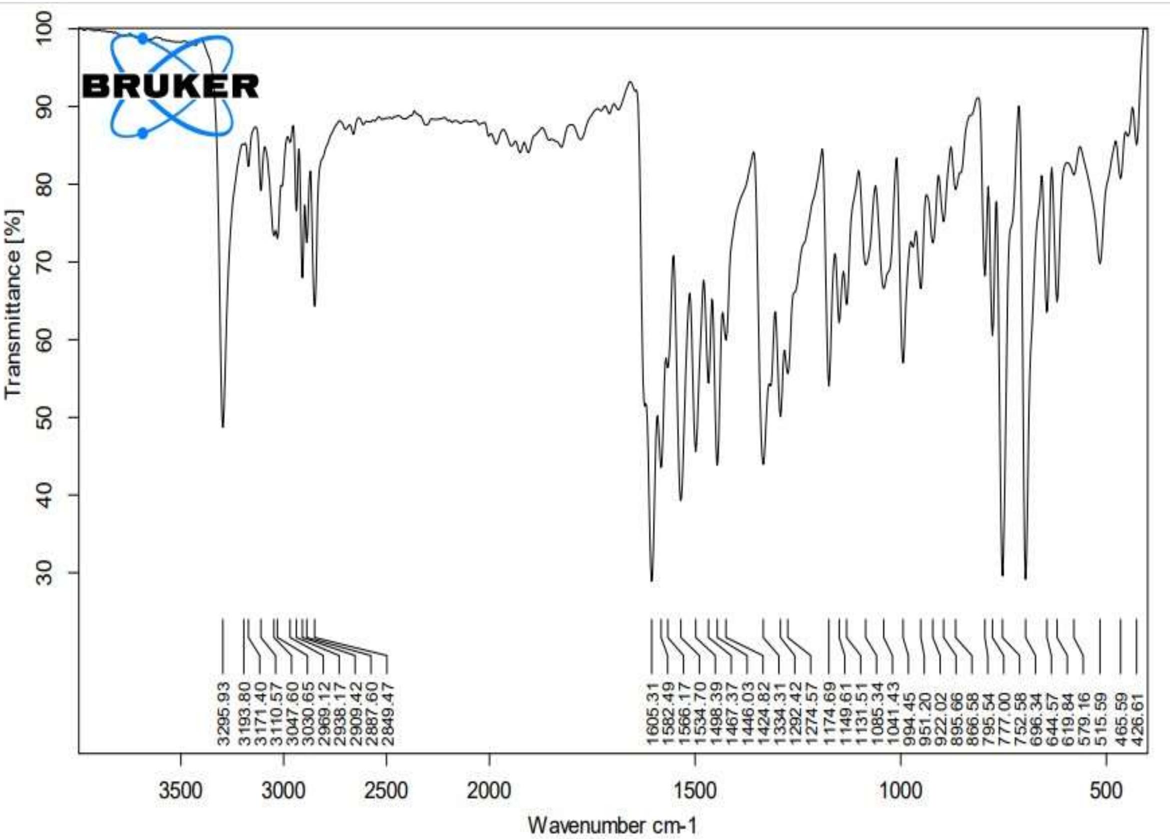

Figure. 2(A).3. IR spectrum of Ligand (L1).

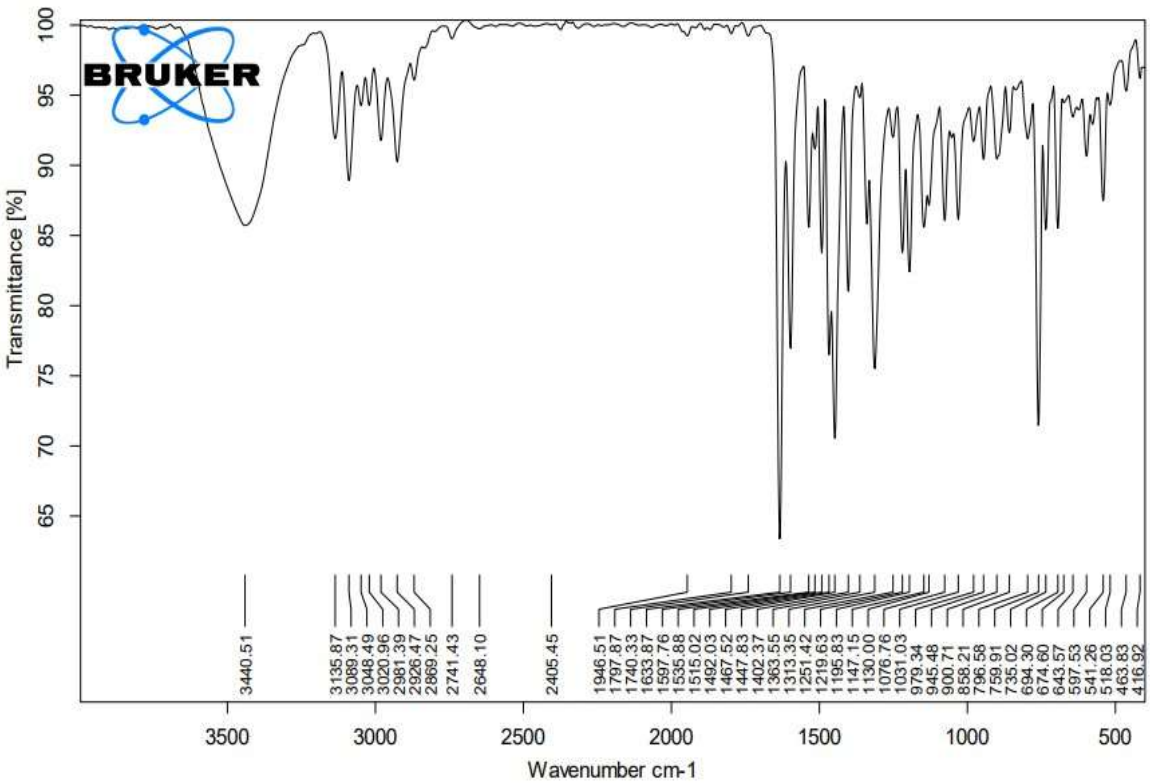

Figure. 2(A).4. IR spectrum of $[Cu(L1)Cl_2]$

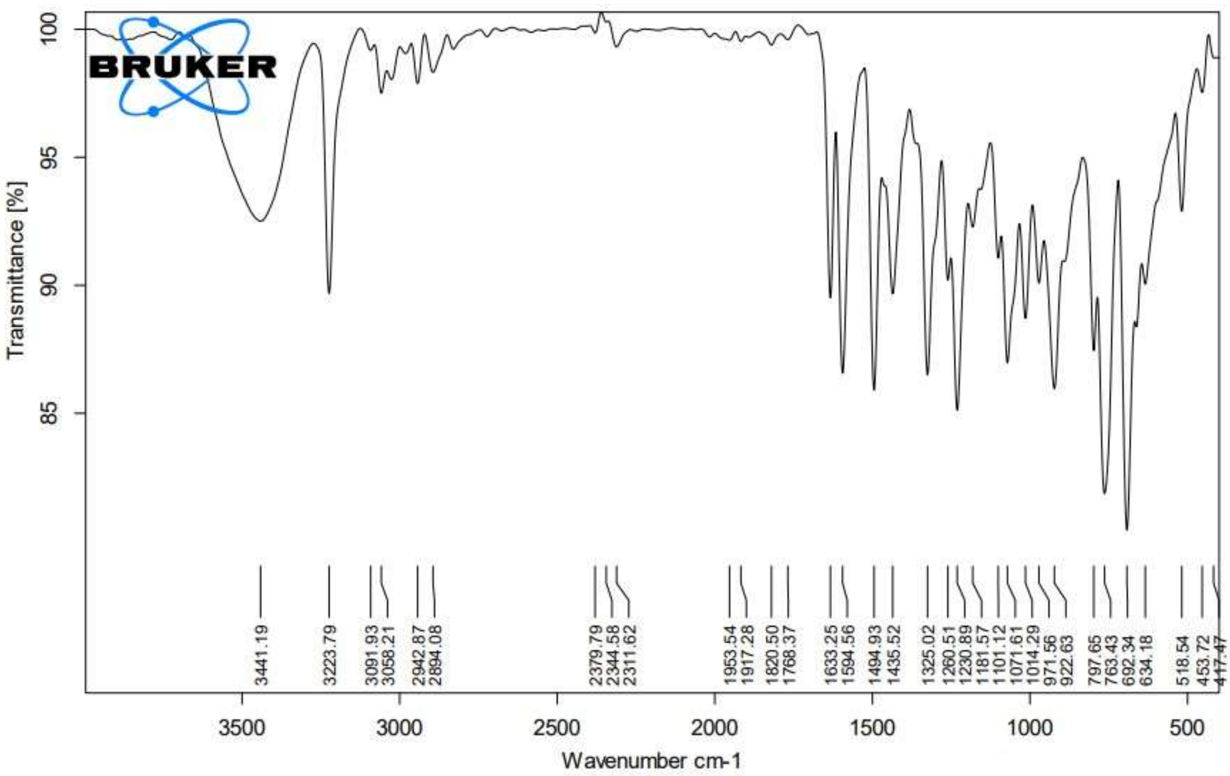

Figure. 2(A).5. IR spectrum of $[Co(L1)Cl_2]$

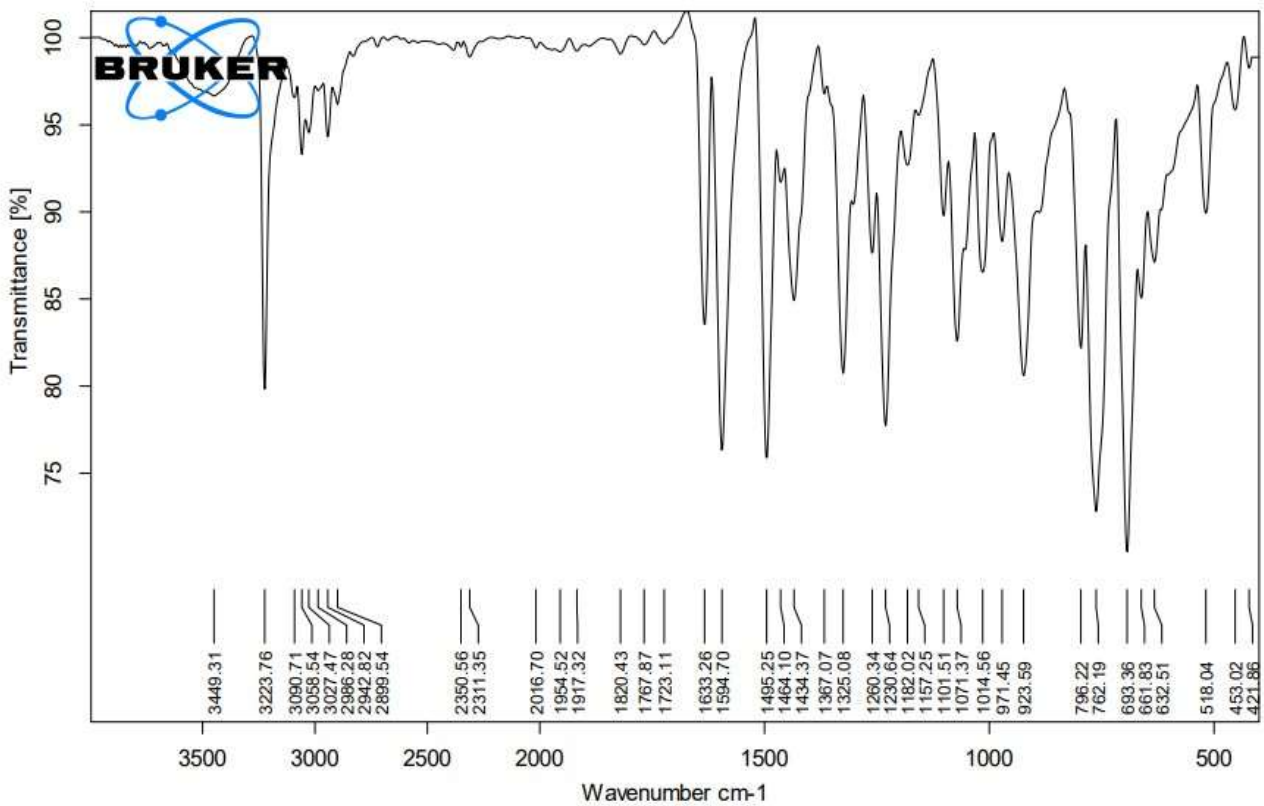

Figure. 2(A).6. IR spectrum of $[Zn(L1)Cl_2]$

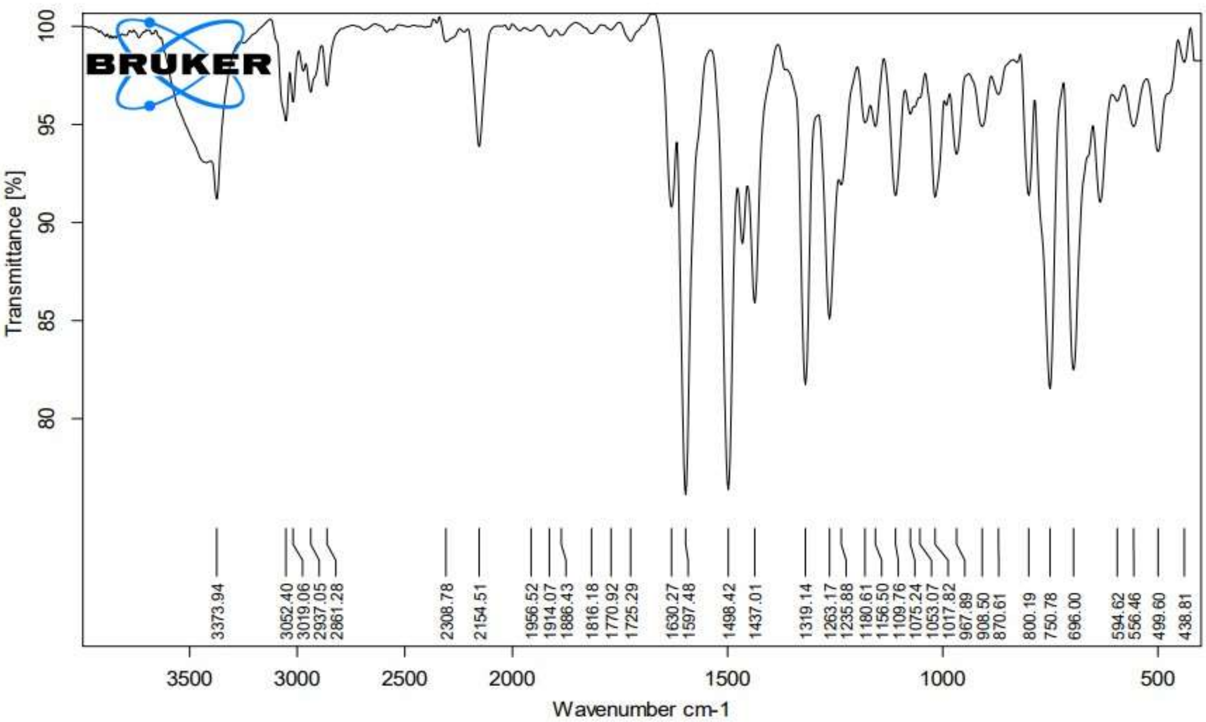

Figure. 2(A).7. IR spectrum of $[Cd(L1)Cl_2]_n$

2(A).4.2.4. Electronic spectral data

The UV-Vis spectra of complexes $[M(L1)Cl_2]$ were recorded in the range of 190 – 850 nm in (1 x 10^{-3} M) CH_3CN. The high intensity bands appeared at less than 400 nm are due to intra ligand n- π* / π - π* transition. In the visible region, a broad absorption band was observed at ~628 nm due to $dxy, dyz \rightarrow dx^2{-}y^2$ transition for copper (II) complex. This type of spectral feature is typical for Cu(II) complexes with square pyramidal geometry. Generally, trigonal bipyramidal Cu(II) complexes show two spectral bands in the region of < 750 nm (due to $d_{xy}, d_{yz} \rightarrow d_{z^2}$) and at > 800 nm (due to $d_{xy}, d_{x^2-y^2} \rightarrow d_{z^2}$) transition [34]. Absence of spectral band in the two regions and presence of one band at 628 nm in the copper compound also support the geometry around copper(II) center is distorted square pyramidal [35]. For Co(II) complex, two broad absorption bands observed at 706 and 501 nm and these were due to d-d transition or ligand field transition. This type of transitions is generally observed for high spin cobalt (II) complexes [35].

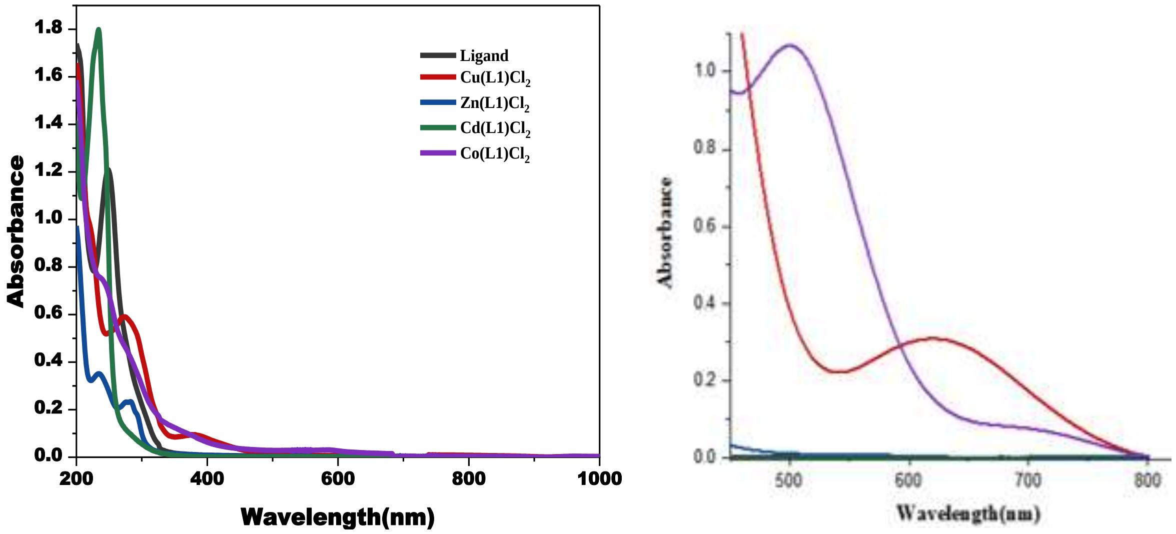

Figure 2(A).8 Electronic spectra of ligand(L1) and complexes in CH_3CN (10^{-3} M).

2(A).4.2.5. Magnetic studies

The room temperature magnetic susceptibility measurement of the complexes show μ_{eff} value for complex **1** is 1.80 BM indicating one electron paramagnetism, whereas μ_{eff} value for complex **2** is 3.84 BM indicating three electrons paramagnetism.

2(A).4.2.6. EPR spectra

The X-band EPR spectrum of Cu (II) complex in the frozen solution (77 K) in DMSO shows four-line splitting with g_{II} = 2.229 and $g_{\perp}$ = 2.021 indicating the interaction of the unpaired electron with nuclear spin of the copper(II) nucleus (^{63,65}Cu; I = 3/2).

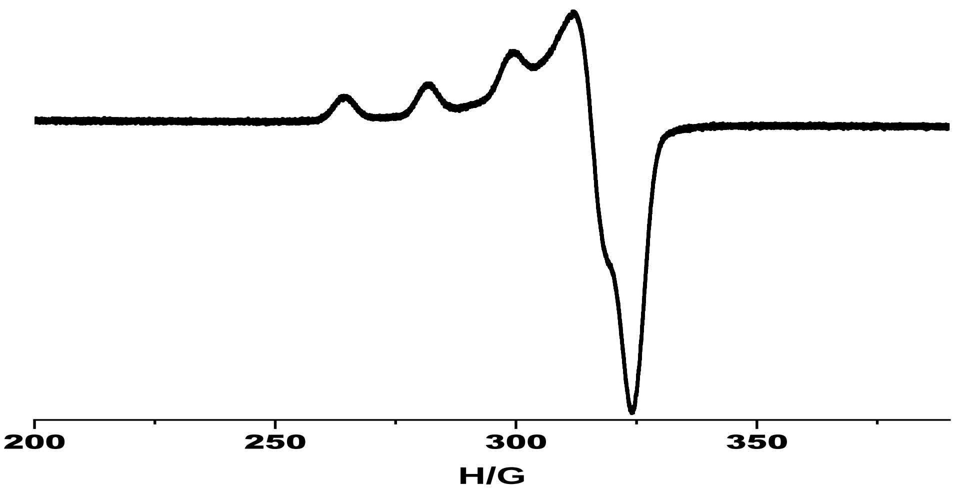

Figure 2(A).9 X-Band EPR spectrum of Cu(II) complex in DMSO at 77 K

2(A).4.3. Descriptions of Crystal Structures

2(A).4.3.1. Crystal structure of the ligand (L1)

ORTEP diagrams with atom numbering schemes of the ligand L1 is shown in [Fig. 2(A).10]. The ligand has crystallized in the monoclinic system with $P2_1/c$ space group. The Schiff base ligand L1 has three nitrogen N1, N2 and N3 coordination sites. In the molecule, H atom of H-N (1) has H-bonded with N3 of pyridine [Fig. 2(A).10(b)].

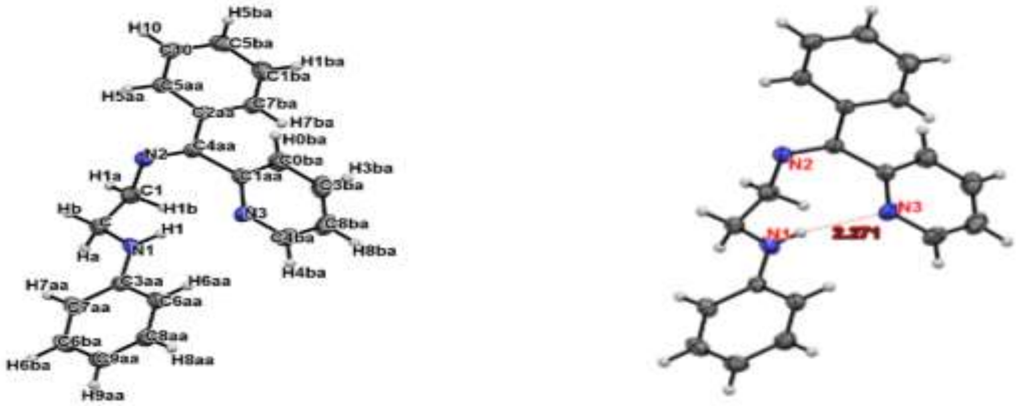

(a) **(b)**

Figure 2(A).10. (a). ORTEP diagram of the ligand L1 (40% probability factor for the thermal ellipsoids**). (b).** H-bonding in the ligand L1.

2(A).4.3.2. Crystal structures of the [M(L1)Cl_2] [M = Cu(II), Co(II) and Zn(II)].

The molecular structures with atom numbering scheme of the complexes **1-3** are shown in Figs. 2(A).11-13 and selected bond lengths and bond angles of the complexes are given in Table 2(A).2 and Table 2(A).3. All the complexes are isotype and crystallized in the monoclinic system with $P2_1/n$ space group. The ligand L1 is neutral and acts as tridentate in the complexes, utilizing its all three nitrogen atoms N1, N2 and N3 for coordination with the metal centres. All the metal centers have five coordination and the coordination environment around the metal centres is MN_3Cl_2 and bonded with N1, N2 and N3 of the ligand L1 and two chloride atoms Cl1 and Cl2. Equatorial and axial bond angles of the complexes show that the coordination geometry around the metal centres are described as distorted square pyramidal geometry [τ= 0.15 to 0.3]. In the complexes, the equatorial positions are occupied by three nitrogen atoms N1, N2, N3 of the ligand L1 and one chlorine atom Cl1 and the axial position is occupied by Cl2 atom. The equatorial bond distances are in the range of 1.198 to 2.259 Å and the axial bond distances are in the range 2.250-2.406 Å. The M-N bond distances are in the range of 1.989-

2.314 Å and the M-Cl bond distances are in the range of 2.250 – 2.406 Å. The M-NH distances in the three complexes are not equal and much longer than M-N bond distances. Unequal bond lengths produce distortion in the molecules.

In all three complexes, one molecule is connected with nearest molecule through short intermolecular interaction between the Cl-atom of one molecule and H-atom of nearest benzene ring of another molecule along b-axis [Table 2(A).4].

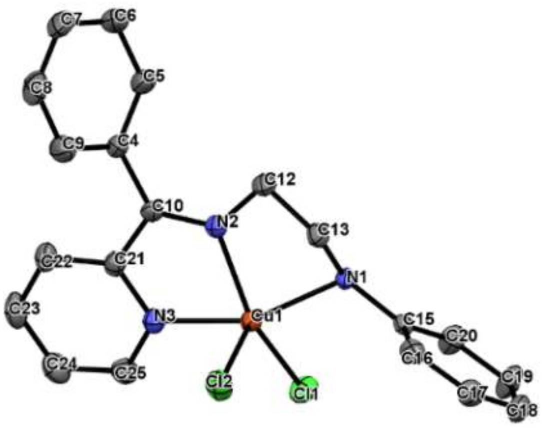

(a)

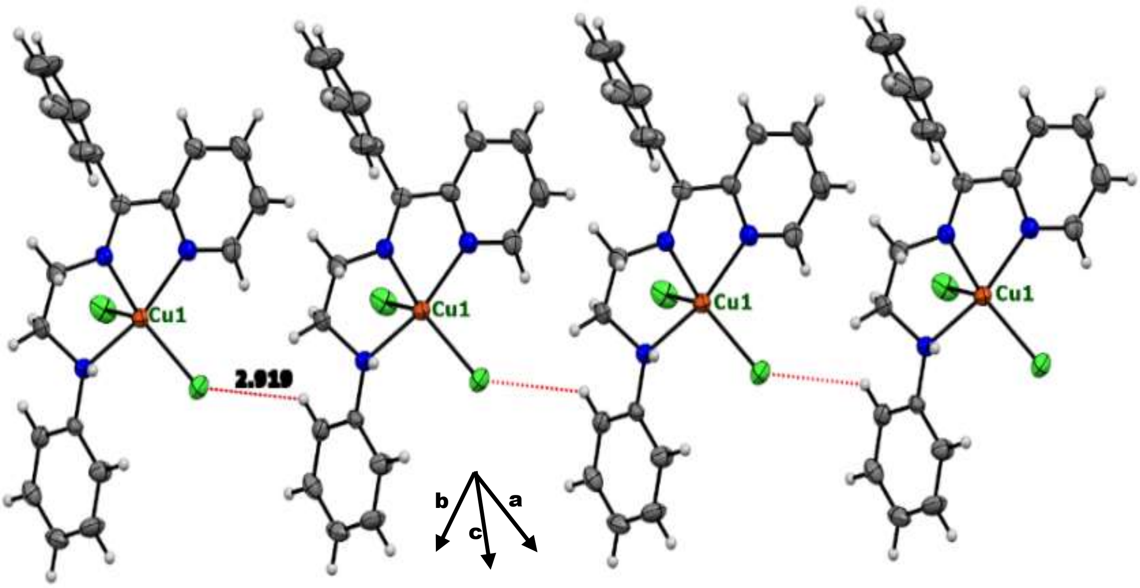

(b)

Figure 2(A).11. (a) ORTEP diagram of the Cu (II) complex with atom numbering scheme (40% probability factor for the thermal ellipsoids). Hydrogen are omitted for clarity.
(b) 1D network of complex **1** through intermolecular interaction.

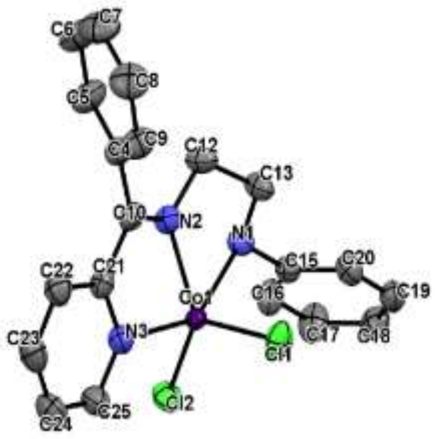

(a)

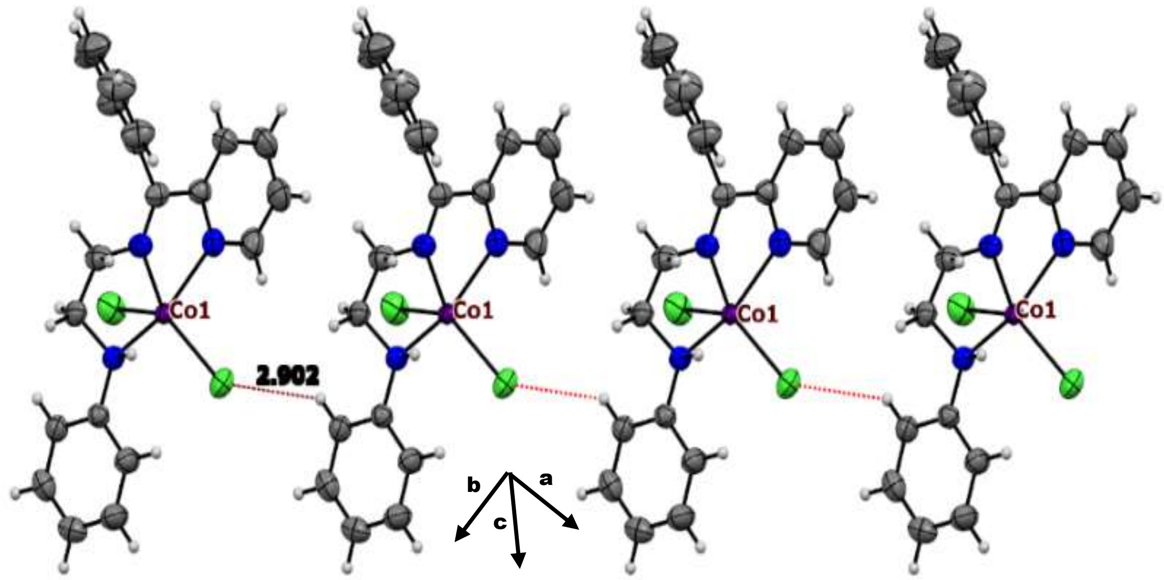

(b)

Figure 2(A).12. (a) ORTEP diagram of the Co (II) complex (40% probability factor for the thermal ellipsoids). H-atoms are omitted for clarity. **(b)** 1D network of Co (II) complex through intermolecular interaction.

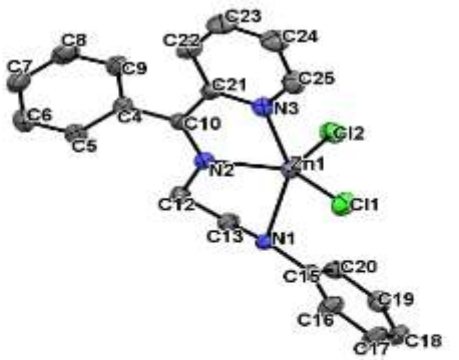

(a)

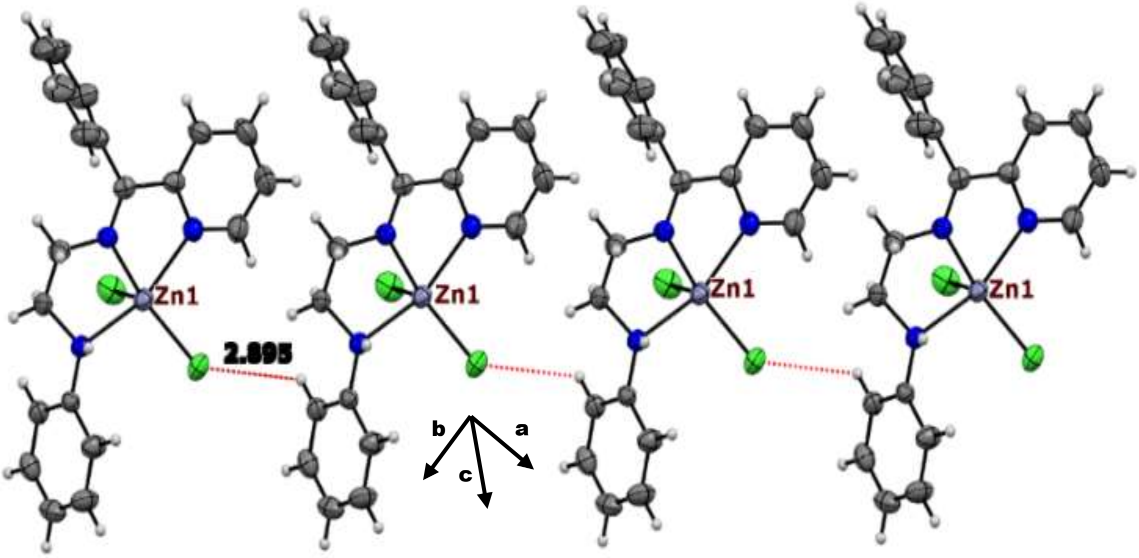

(b)

Figure 2(A).13. (a) ORTEP diagram of the Zn (II) complex (40% probability factor for the thermal ellipsoids). Hydrogen atoms are omitted for clarity**.**
(b) 1D network of Zn (II) complex through intermolecular interaction.

2(A).4.3.3. Crystal structure of $[Cd(L1)Cl_2]_n$

The ORTEP diagrams of Cd (II) complex is shown in Fig. 2(A).14. The Cd (II) complex crystallizes in triclinic crystal system with space group P-1. The asymmetric unit of Cd(II) complex [Fig.2(A).14(a)] consists of one cadmium(II) ion, two nitrogen atoms of the Schiff base ligand and four Cl atoms. This structure consists of polymeric chain of Cd atoms and two Cd centres are bonded by two bridging chloride ions as Cd-$(Cl)_2$-Cd chain and produce four membered ring. Each Cd centres has $CdCl_4N_2$ coordination environment with octahedral geometry and surrounded by two nitrogen atoms N2 and N3 of the Schiff base ligand L1 and four bridging Cl atoms. Two Cd-N bond distances of the ligand L1 are nearly equal (2.350 and 2.382 Å) but four Cd-Cl bonds (2.519, 2.566, 2.628 and 2.795 Å) are not equal and they are much longer than Cd-N bond length of the ligand L1. The distance between the two cadmium centres i.e. Cd-$(Cl)_2$-Cd distance is 3.699 Å. Long and unequal bond lengths produce distortion in the molecule. The equatorial positions of the Cd atom occupied by Cl1, Cl2 of the bridging chloride, Cl2 of another bridged Cd atom and N2 of the ligand and the axial positions are occupied by N3 of the ligand L1 and Cl2 of the second bridged. Ligand L1 acts as bidentate ligand in the molecule. The bridging nature of Cl atoms i.e. μ-Cl give 1D polymeric zig-zag chain along b-axis.

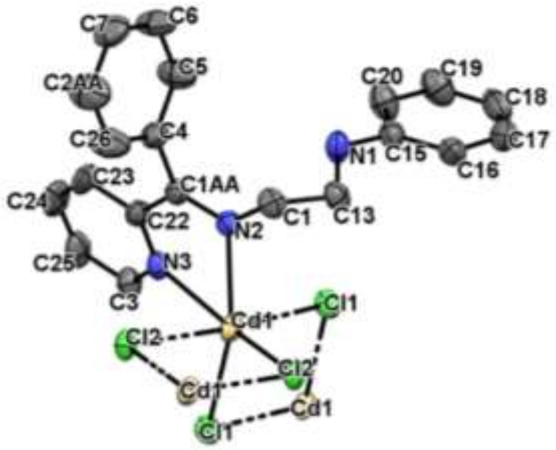

(a)

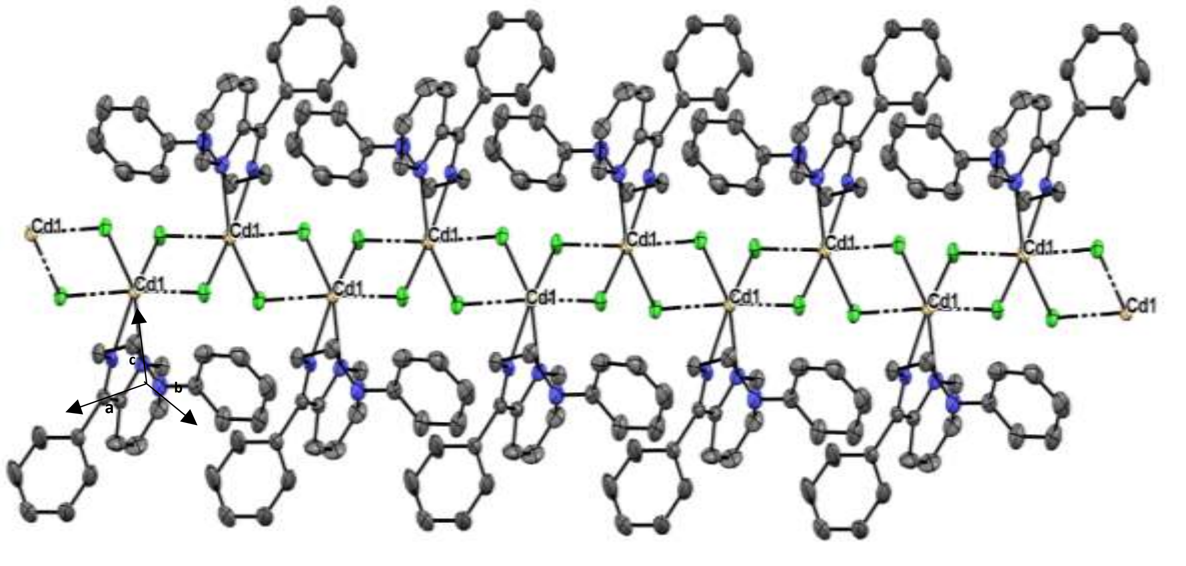

(b)

Figure 2(A).14. (a) ORTEP diagram of asymmetric unit of polymeric complex $[Cd(L)Cl_2]_n$ with atom numbering scheme. H-atoms are omitted for clarity. **(b)** The 1D polymeric zig-zag chain of Cd (II) complex.

Table 2(A).2 Selected bond lengths (A°) for ligand(L1) and complexes

Ligand(L1)		$[Cu(L1)Cl_2]$		$[Co(L1)Cl_2]$		$[Zn(L1)Cl_2]$		$[Cd(L1)Cl_2]_n$	
N(2)-C(4aa)	1.276(2)	Cu(1)-Cl(1)	2.258(9)	Co(1)-Cl(2)	2.251(11)	Zn(1)-Cl(1)	2.250(9)	Cd(1)-Cl(2^1)	2.794(18)
N(2)-C(1)	1.461(2)	Cu(1)-Cl(2)	2.407(10)	Co(1)-Cl(1)	2.252(12)	Zn(1)-Cl(2)	2.252(9)	Cd(1)-Cl(1^2)	2.628(18)
N(1)-C(3aa)	1.372(2)	Cu(1)-N(3)	2.036(3)	Co(1)-N(2)	2.116(3)	Zn(1)-N(2)	2.112(2)	Cd(1)-Cl(1)	2.566(2)
N(1)-C	1.437(2)	Cu(1)-N(1)	2.109(3)	Co(1)-N(3)	2.179(3)	Zn(1)-N(3)	2.179(3)	Cd(1)-N(2)	2.382(6)
N(3)-C(1aa)	1.334(2)	Cu(1)-N(2)	1.989(3)	Co(1)-N(1)	2.311(3)	Zn(1)-N(1)	2.304(2)	Cd(1)-N(3)	2.350(5)
								Cd(1)-Cl(2)	2.519(17)

Table 2(A).3 Selected bond angles (º) for ligand(L1) and complexes

Ligand(L1)		$[Cu(L1)Cl_2]$		$[Co(L1)Cl_2]$	
C(1)-N(2)-C(4aa)	121.80(15)	Cl1-Cu(1)-Cl(2)	112.01(4)	Cl(1)-Co(1)-Cl(2)	119.50(5)
C-N(1)-C(3aa)	124.23(14)	N(3)-Cu(1)-Cl(1)	96.24(8)	N(2)-Co(1)-Cl(2)	138.17(10)
C(0ba)-C(1aa)-C(4aa)	121.78(16)	N(3)-Cu(1)-Cl(2)	96.62(8)	N(2)-Co(1)-Cl(1)	102.31(10)
N(3)-C(1aa)-C(4aa)	115.71(15)	N(1)-Cu(1)-Cl(1)	96.38(8)	N(3)-Co(1)-Cl(2)	96.74(9)
N(3)-C(1aa)-C(0ba)	122.50(16)	N(1)-Cu(1)-Cl(2)	95.19(9)	N(3)-Co(1)-Cl(1)	101.10(10)
		N(3)-Cu(1)-N(1)	158.06(12)	N(2)-Co(1)-N(3)	75.17(13)
		N(2)-Cu(1)-Cl(1)	148.59(9)	Cl(2)-Co(1)-N(1)	95.39(8)
		N(2)-Cu(1)-Cl(2)	99.39(8)	Cl(1)-Co(1)-N(1)	98.74(9)
		N(2)-Cu(1)-N(3)	78.92(11)	Co(1)-N(2)-N(1)	75.80(12)
		N(2)-Cu(1)-N(1)	80.95(11)	Co(1)-N(3)-N(1)	147.64(13)

[Zn(L1)Cl$_2$]		**[Cd(L1)Cl$_2$]$_n$**	
Cl(1)-Zn(1)-Cl(2)	119.49(4)	Cl(2)-Cd(1)-Cl(1^2)	97.68(6)
Cl(1)-Zn(1)-N(1)	95.49(6)	Cl(2)- Cd(1)-Cl(1)	100.47(7)
Cl(2)-Zn(1)-N(1)	98.49(7)	Cl(1^2)$^-$ Cd(1)-- Cl(1^2)	175.89(6)
N(2-Zn(1)-Cl(1)	138.18(7)	Cl(1)- Cd(1)-Cl(2^1)	93.19(6)
N(2)-Zn(1)-Cl(2)	102.31(7)	Cl(1)- Cd(1)- Cl(1^2)	89.19(6)
N(2)-Zn(1)-N(3)	75.15(10)	N(2)- Cd(1)- Cl(2^1)	82.41(13)
N(2)-Zn(1)-N(1)	75.93(9)	N(2)- Cd(1)-Cl(2)	94.77(15)
N(3)-Zn(1)-Cl(1)	96.72(7)	N(2)- Cd(1)- Cl(1^2)	94.38(14)
N(3)-Zn(1)-Cl(2)	101.09(7)	N(2)- Cd(1)-Cl(1)	163.74(15)
N(3)-Zn(1)-N(1)	147.85(10)	N(3)- Cd(1)- Cl(2)	160.81(17)

Table 2(A).4 Intermolecular interactions of the complexes.

Compound/D-H----A	D-H (A^o)	H---A (A^o)	D---A (A^o)	D-H---A (^{o})
[Cu(L1)Cl$_2$] (1)				
Cl1-H16-C17	2.919	0.930	3.478	119.82
Cl2-H6-C6	2.765	0.929	3.653	160.01
Cl2-H22-C22	2.950	0.230	3.601	128.35
[Co(L1)Cl$_2$] (2)				
Cl2-H20-C20	2.902	0.929	3.468	120.61
Cl1-H6-C6	2.763	0.930	3.648	169.42
[Zn(L1)Cl$_2$] (3)				
Cl1-H20-C20	2.895	0.830	3.487	120.98
Cl2-H6-C6	2.757	0.830	3.642	159.18

2(A).4.4. Antimicrobial activity study

The ligand and the derived complexes were evaluated for their antimicrobial activity Table 2(A).5. Negative control plate lacked zone of inhibition while strong inhibition was observed in the presence of chloramphenicol control, which proved the susceptibility of microorganisms to antimicrobial agents. Ligand L1 was found to inhibit the growth of only *E. coli* (MIC = 10 mM) and the derived complexes from this ligand possessed antimicrobial activity with variable selectivity for tested microorganisms. $[Co(L1)Cl_2]$ and $[Cd(L1)Cl_2]_n$ were found to act against Gram positive bacteria only, where $[Co(L1)Cl_2]$ was active against *S. aureus* (MIC = 10 mM) only and $[Cd(L1)Cl_2]_n$ displayed activity against *B. subtilis* (MIC = 5 mM) with significantly high activity against *S. aureus* (MIC = 0.5 mM). $[Zn(L1)Cl_2]$ along with activity against Gram positive *S. aureus* and *B. subtilis* (MIC = 5 mM), exhibited activity against Gram negative *E. coli* (MIC = 10 mM). $[Cu(L1)Cl_2]$ was observed to exhibit antimicrobial activity against all the tested microorganisms, with relatively more antimicrobial activity against both *S. auerus* and *B. subtilis* (MIC = 5 mM) than against Gram negative *E. coli* and *P. vulgaris* (MIC=10 mM). Whereas Kuzmanović et al. [36] showed the ligand type was the factor determining antimicrobial activity of the complexes, evaluation of the antimicrobial activity of complexes obtained by switching central metal ions against a single ligand in our work demonstrated that the metal ion is another important parameter that decides antimicrobial activity of the coordination complex. Considering all the mechanistic frameworks currently known for antimicrobial activity of metals [37], it is understood that the antimicrobial activity of Cu complex is the result of the ability of Cu to catalyse the Fenton chemistry better than Cd, Zn and Co complex, which demonstrated activity against both Gram positive and Gram negative bacteria is one such desired antimicrobial agent. The work provide basis to design compounds in which both the metal and ligand partners act synergistically to improve the overall activity of the antimicrobial compounds. Complexation of the metal ion reduces the polarity of the metal ion, which eventually increases the lipophilicity of the complex, a factor governing the ability of the antimicrobial agent to go past the microbial plasma membrane composed of phospholipid bilayer [38]. Altogether the complexes were found to target more effectively Gram-positive bacteria than Gram-negative bacteria. This can be attributed to the structural differences in the cell wall between the Gram-positive and Gram-negative bacteria.

Table 2(A).5 Antimicrobial activity of the Schiff base ligand(L1) and its metal complexes.

Compound	**MIC value in mM**			
	E. coli	***P. vulgaris***	***S. aureus***	***B. subtilis***
Ligand	>10	>10	10	>10
$[Cu(L)Cl_2]$	5	5	10	10
$[Co(L)Cl_2]$	>10	10	>10	>10
$[Zn(L)Cl_2]$	5	5	10	>10
$[Cd(L)Cl_2]_n$	5	0.5	>10	>10
Chloramphenicol	0.0003	0.0015	0.0015	0.003

#MIC in mM

*E. coli – Escherichia coli gram -ve

*P. vulgaris – Proteus vulgaris gram -ve

*S. aureus – Staphylococcus aureus gram +ve

*B. subtilis – Bacillus subtilis gram +ve.

The latter carries an additional outer envelope of lipopolysaccharides, which foils the treatment efforts against it. Additionally, the growing numbers of multi-drug resistant strains particularly from Gram-negative group is a matter of global concern. Therefore, attempts are being made to discover new agents which can target both Gram-negative and Gram-positive bacteria effectively. From our study, copper-containing complex $[Cu(L1)Cl_2]$ which demonstrated activity against both Gram-positive and Gram-negative bacteria is one such desired antimicrobial agent. The work provides basis to design compounds in which both the metal and ligand partners act synergistically to improve the overall activity of the antimicrobial compounds.

2(A).5. Conclusion

Mononuclear Cu(II), Co(II) and Zn(II) and polynuclear Cd(II) complexes have been synthesized with N_3-donor Schiff base ligand L1 and characterized. Structural data shows that mononuclear complexes of Cu(II), Co(II) and Zn(II) have distorted square pyramidal geometry and polynuclear Cd(II) complex has octahedral geometry. Cd(II) forms 1D coordination polymer through bridging Cd-(μ-Cl)$_2$-Cd linkage. Antimicrobial studies demonstrated the antimicrobial potential of the tested complexes **1**, **2**, **3** and **4** against Gram negative and Gram positive bacteria. Copper(II) complex was found to effectively target both Gram positive and Gram negative bacteria and it is therefore put forward as a promising antimicrobial agent.

2(A).6. References

1. M. S. More, P. G. Joshi, Y. K. Mishra, P. K. Khanna. Mater. Today Chem. 14 (2019) 100195.
2. J. Zhang, L. Xu, W. Y. Wong. Coord. Chem. Rev. 355 (2018) 180.
3. A. Kajal, S. Bala, S. Kamboj, N. Sharma, V. Saini. J. Catalysts (2013) 1.
4. M. N. Uddin, S. S. Ahmed, S. M. R. Alam. J. Coord. Chem.73 (2020) 3109.
5. A. Abu-Dief, I. Mohamed. Beni-Suef Univ. J. Basic and Applied Sci. 4 (2015) 119.
6. M. Ghorbanloo, R. Bikas, S. Jafari, M. S. Krawczyk, T. Lis. J. Coord. Chem. 71 (2018) 1510.
7. R. Samimi, H. Golchoubian. Transition Met. Chem. 42 (2017) 643.
8. S. H. Rahaman, H. Chowdhury, D. Bose, R. Ghosh, C. H. Hung, B. K. Ghosh. Polyhedron 24 (2005) 1755.
9. S. Ray, S. Konar, A. Jana, A. Dhara, K. Das, S. Chatterjee, M. S. El Fallah, J. Ribas, S. Kumar Kar. Polyhedron 68 (2014) 212.
10. K. Jana, S. Das, H. Puschmann, S. C. Debnath, A. Shukla, A. K. Mahanta, M. Hossain, T. Maity, B. C. Samant. Inorg. Chim. Acta 487 (2019) 128.
11. E. Manoj, M. R. P. Kurup, A. Punnoose. Spect. Chim. Acta A 72 (2009) 474.
12. S. H. Rahaman, H. K. Fun, B. K. Ghosh. Polyhedron 24 (2005) 3091.
13. P. Bera, A. Aher, P. Brandao, S. Manna, I. Bhattacharyyaa, C. Pramanik, B. Mondal, S. Das, P. Bera. J. Mol. Struct. 1224 (2021) 129015
14. M. Li, S. Huang, C. Ye, Y. Xie. Spect. Chim. Acta. A 150 (2015) 290.
15. S. Roy, S. Kundu, K. Bhar, S. Satapathi, P. Mitra, B. K. Ghosh. Ind. J. Chem. 52A (2013) 34.
16. S. Kundu, S. Roy, K. Bhar, D. Sutradhar, P. Mitra, B. K. Ghosh. Ind. J. Chem. 52A (2013) 1404.
17. S. Satapathi, S. Choubey, S. Das, K. Bhar, R. Ghosh, P. Mitra, B. K. Ghosh. J. Chem. Cryst. 42 (2012) 1060.
18. B. Biswas, A. Pal, G. R. Krishna, C. M. Reddy, F. Tuna, R. Ghosh. Polyhedron 30 (2011) 2032.
19. M. E. Hossain, M. N. Alam, J. Begum, M. A. Ali, M. Nazimuddin, F. E. Smith, R. C. Hynes. Inorg. Chim. Acta 249 (1996) 207.

20. Y. K. Abdel-Monem, S. A. Abouel-Enein, S. M. El-Seady. J. Mol. Struct. 1152 (2018) 115.
21. S. Mandal, T. K. Karmakar, A. Ghosh, M. Fleck, D. Bandyopadhyay. Polyhedron 30 (2011) 790.
22. M. X. Li, L. Z. Zhang, C. L. Chen, J. Y. Niu, B. S. Ji. J. Inorg. Biochem. 106 (2012) 117.
23. A. A. S. Al-Hamdani, W. Al Zoubi. Spect. Chim. Acta A 137 (2014) 75.
24. W. Clegg, R. W. Harrington, K. Barati, M. H. Habibi, M. Montazerozohori, A. Lalegani. Acta Cryst. C71 (2015) 578.
25. S. Mondal, M. Chakraborty, A. Mondal, B. Pakhira, A. J. Blake, E. Sinn and S. K. Chattopadhyay. New J. Chem. 42 (2018) 9588.
26. P. Bhowmik, S. Chattopadhyay, M. G. B. Drew, C. Diaz, A. Ghosh. Polyhedron 29 (2010) 2637.
27 A. Z. El-Sonbati, W. H. Mahmoud, G. G. Mohamed, M. A. Diab, S. M. Morgan, S. Y. Abbas. Appl. Organomet. Chem. (2019) 33e5048.
28. Agilent, CrysAlis PRO. Agilent Technologies UK Ltd, Yarnton, England (2011).
29. G. M. Sheldrick. SAINT, 5.1st edn. Siemens Industrial Automation Inc., Madison, WI (1995).
30. G. M. Sheldrick. SHELXL 97 Program for Crystal Structure Refinement, University of Gottingen, Gottingen (1997).
31. L. J. Farrugia. J. Appl Cryst. 32 (1999) 837.
32. L. J. Farrugia. J. Appl. Cryst. 30 (1997) 565.
33. M. H. Sadhu, S. B. Kumar, J. K. Saini, S. S. Purani, T. R. Khanna. Inorg. Chim. Acta 466 (2017) 219.
34. U. Mukhopadhyay, I. Bernal, S. S. Massoud, F. A. Mautner. Inorg. Chim. Acta 357 (2004) 3673.
35. A. Solanki, S. B. Kumar, A. A. Doshi, C. Ratna Prabha. Polyhedron 63 (2013) 147.
36. S. O. Podunavac-Kuzmanovic, V. M. Leovac, D. D. Cvetkovic. J. Serb. Chem. Soc. 73 (2008) 153.
37. J. A. Lemire, J. J. Harrison, R. J. Turner. Nature Reviews Microbiology 11 (2013) 371.
38. J. Devi, N, Batra, R. Malhotra. Spectro. Chim. Acta. A 97 (2012) 397.

CHAPTER-2(B)

Mononuclear Octahedral Metal (II) complexes containing tridentate N-donor Schiff base ligand: syntheses, structures and cytotoxic activity.

Abstract

A series of six octahedral mononuclear metal complexes of the type $[M(L1)_2](ClO_4)_2.2H_2O$ where M = Cu(II), Ni(II), Mn(II), Co(II), Zn(II) and Cd(II) were synthesized with tridentate N_3-donor Schiff base ligand N′-Phenyl-N″(phenyl(pyridin-2-yl)methylene)ethane-1,2-diamine(L1) and characterized by elemental analysis, IR, mass spectra, electronic spectra, conductivity measurement and magnetic study. Single crystal X-ray diffraction study of the two complexes $[Ni(L1)_2](ClO_4)_2.2H_2O$ and $[Zn(L1)_2](ClO_4)_2.2H_2O$ showed both the complexes have distorted octahedral geometry. Cytotoxic activity of the complexes showed dose depended toxicity and Cu(II) and Mn(II) complexes have very low IC50 value among the complexes.

2(B).1. Introduction

Transition metal complexes using Schiff bases have been an important area of research in coordination chemistry since long time due to their wide range of applications in many areas such as catalysis, magnetic and biological activities including antifungal, antibacterial, antiviral and antipyretic properties etc. [1-15]. There are many reports on transition metal complexes using multidentate Schiff base ligands with different donor atoms and they have played an important role in the development of synthetic inorganic chemistry and have wide range of applications [16-28].

As a part of our research on synthesis and structural characterization of transition metal complexes with Schiff base ligands, we have reported mononuclear three coordinated complexes $[M(L1)Cl_2]$ [where M= Cu(II), Co(II) and Zn(II)] and one octahedral polynuclear complex $[Cd(L1)Cl_2]_n$ with Schiff base ligand N′-Phenyl-N″(phenyl(pyridin-2-yl)methylene)ethane-1,2-diamine (L1) and studied their antimicrobial activities [29]. In this paper, we report on the syntheses, characterization and crystal structures of mononuclear octahedral complexes $[M(L1)_2](ClO_4)_2$ [M= Cu(II), Co(II), Mn(II), Ni(II), Zn(II) and Cd(II)] with ligand N′-Phenyl-N″(phenyl(pyridin-2-yl)methylene)ethane-1,2-diamine (L1) and studied their cytotoxic activities.

2(B).2. Experimental

2(B).2.1. Materials

The chemicals and solvents were analytical grade and purchased from commercial sources. N-phenylethene-1,2-diamine, 2-benzoylpyridine (Aldrich) were reagent grade and used as received. The ligand N′-Phenyl-N″(phenyl(pyridin-2-yl)methylene)ethane-1,2-diamine(L1) was synthesized as per reported method [29]. Metal perchlorate hexahydrate were prepared by the reaction of metal carbonates with dilute $HClO_4$ acid and followed by evaporation of the solution on steam bath.

2(B).2.2. Syntheses of complexes

2(B).2.2.1. $[Cu(L1)_2](ClO_4)_2.2H_2O$ (1)

To a stirring solution of copper (II) perchlorate hexahydrate (0.092 g, 0.25 mmol) in methanol (10 mL) was added a solution of ligand L1 (0.150 g, 0.50 mmol) dissolved in the same solvent

(10 mL). Colour of the solution changed to dark green colour immediately. The solution was stirred for additional 3h, filtered and the filtrate was left to evaporate slowly at room temperature. Green compound was obtained after 2 days.

Yield. 0.146 g (65%). Found C = 53.00, H = 4.49, N = 9.50%, Elemental analysis calc. for $C_{40}H_{42}N_6O_{10}Cl_2Cu$: C = 53.33, H = 4.66, N = 9.32%. IR (KBr pellet) cm^{-1}; ν(N-H), 3284s; ν (C=N), 1630s; ν(C=C)+ ν(C=N)py, 1598m; ν(C=C)ph, 1493m; ν(M-N), 528vw; ν(ClO_4^-), 1068br; δ(O-Cl-O), 623s. λ_{max}/nm (ε_{max}/$mol^{-1}cm^{-1}$): 650(441), 402(570), 290(3880), 221(6845). MS (ESI): m/z = 663.71 (100%) $[C_{40}H_{42}N_6O_{10}Cl_2Cu]^+$. $\Lambda_M(CH_3CN)$ ($\Omega^{-1}cm^2mol^{-1}$) = 246. μ_{eff} = 1.82 BM.

2(B).2.2.2. $[Ni(L1)_2](ClO_4)_2.2H_2O$ (2)

To a stirring solution of nickel (II) perchlorate hexahydrate (0.091 g, 0.25 mmol) in methanol (10 mL) was added a solution of ligand L1 (0.150 g, 0.50 mmol) dissolved in methanol (10 mL). Colour of the solution changed to dark brown colour immediately and the solution was stirred for additional 3 h. Filtered the solution and the filtrate was left to evaporate slowly at room temperature. Square shape brown crystals were obtained after 2-3 days.

Yield. 0.135 g (60%). Found C = 56.07, H = 4.49, N = 9.95 %, Elemental analysis calc. for $C_{40}H_{42}N_6O_{10}Cl_2Ni$: C = 56.27, H = 4.68, N = 10.17. IR (KBr pellet) cm^{-1}; ν(N-H), 3229s; ν(C=N), 1635s; ν(C=C)+ ν(C=N)py, 1598m; ν(C=C)ph, 1493m; ν(M-N), 530vw; ν(ClO_4^-), 1105br; δ(O-Cl-O), 623s. λ_{max}/nm (ε_{max}/$mol^{-1}cm^{-1}$): 841(275), 521(617), 280(4459), 245(5114), 225(6460). $\Lambda_M(CH_3CN)$($\Omega^{-1}cm^2mol^{-1}$) = 243. μ_{eff} = 2.75 BM.

2(B).2.2.3. $[Mn(L1)_2](ClO_4)_2.2H_2O$ (3)

To a stirring solution of manganese (II) perchlorate hexahydrate (0.090 g, 0.25 mmol) in methanol (10 mL) was added a solution of ligand L1 (0.150 g, 0.50 mmol) dissolved in the same solvent (10 mL). The colour of the solution was changed from light colour to brown colour immediately and dark brown coloured solution was stirred for additional 3 h, filtered and the filtrate was left to evaporate slowly at room temperature. Rectangular shape light brown small crystals were obtained within 2 days.

Yield. 0.152 g (68%). Found C = 53.13, H = 4.43, N = 9.02%, Elemental analysis calc. for $C_{40}H_{42}N_6O_{10}Cl_2Mn$: C = 52.89, H = 4.62, N = 9.25%. IR (KBr pellet) cm^{-1}; ν(N-H), 3258s; ν(C=N), 1630s; ν(C=C)+ ν(C=N)py, 1598m; ν(C=C)ph, 1493m; ν(M-N), 524 vw; ν(ClO_4^-), 1098br; δ(O-Cl-O), 623s. λ_{max}/nm (ε_{max}/$mol^{-1}cm^{-1}$): 380(1560), 283(5750, 233(9473). MS

(ESI): m/z = 656.96 (100%) $[C_{40}H_{42}N_6O_{10}Cl_2Mn]^+$. $\Lambda_M(CH_3CN)(\Omega^{-1}cm^2mol^{-1})$ = 225. μ_{eff} = 5.80 BM.

2(B).2.2.4. $[Co(L1)_2](ClO_4)_2.2H_2O$ (4)

To a stirring solution of cobalt (II) perchlorate hexahydrate (0.091g, 0.25 mmol) in methanol (10 mL) was added a solution of ligand L1 (0.150 g, 0.50 mmol) dissolved in the same solvent (10 mL). The solution changed to dark purple colour immediately. The solution was stirred for additional 3h, filtered and the filtrate was left to evaporate slowly at room temperature. After 2-3 days, purple colour compound was obtained.

Yield. 0.165 g (75%). Found C = 53.32, H = 4.58, N = 9.62%, Elemental analysis calc. for $C_{40}H_{42}N_6O_{10}Cl_2Co$: C =53.57, H = 4.68, N = 9.37 %. IR (KBr pellet) cm^{-1}; ν(N-H), 3214s; ν(C=N), 1619s; ν(C=C)+ ν(C=N)py, 1598m; ν(C=C)ph, 1490m; ν(M-N), 555vw; $\nu(ClO_4^-)$, 1095br; δ(O-Cl-O), 623s. λ_{max}/nm (ε_{max}/$mol^{-1}cm^{-1}$): 568(475), 469(418), 363(1109), 282 (2761). MS (ESI): m/z = 659.88 (100%) $[C_{40}H_{42}N_6O_{10}Cl_2Co]^+$. $\Lambda_M(CH_3CN)$ $(\Omega^{-1}cm^2mol^{-1})$ = 235. μ_{eff} = 3.87 BM.

2(B).2.2.5. $[Zn(L1)_2](ClO_4)_2.2H_2O$ (5)

To a stirring solution of zinc (II) perchlorate hexahydrate (0.093g, 0.25 mmol) in methanol (10 mL) was added a solution of ligand L1 (0.150 g, 0.50 mmol) dissolved in the same solvent (10 mL). Colourless solution changed to light pale yellow colour immediately. The solution was stirred for additional 3h, filtered and the filtrate was left to evaporate slowly at room temperature. Small square platted yellow crystal were obtained within 2 days.

Yield. 0.157 g (70%). Found C = 53.35, H = 4.53, N = 9.46%, Elemental analysis calc. for $C_{40}H_{42}N_6O_{10}Cl_2Zn$: C = 53.19, H = 4.65, N = 9.30%. IR (KBr pellet) cm^{-1}; ν(N-H), 3244s; ν(C=N), 1639s; ν(C=C)+ ν(C=N)py, 1598m; ν(C=C)ph,, 1493m; ν(M-N), 526vw; $\nu(ClO_4^-)$, 1105br; δ(O-Cl-O), 623s. λ_{max}/nm (ε_{max}/$mol^{-1}cm^{-1}$): 294(4075), 284(5230), 230(8002). MS (ESI): m/z = 665.25 (100%) $[C_{40}H_{42}N_6O_{10}Cl_2Zn]^+$. $\Lambda_M(CH_3CN)$ $(\Omega^{-1}cm^2mol^{-1})$ = 236.

2(B).2.2.6. $[Cd(L1)_2](ClO_4)_2.2H_2O$ (6)

To a stirring solution of cadmium(II) perchlorate hexahydrate (0.104 g, 0.25 mmol) in methanol (10 mL) was added a solution of ligand L1 (0.150 g, 0.50 mmol) dissolved in the same solvent (10 mL). Colourless solution changed to light pale yellow colour immediately. The solution was stirred for additional 3h, filtered and the filtrate was left to evaporate slowly at room temperature. Small white needle crystals were collected after 2 days

Yield. 0.154 g (65%). Found C = 50.12, H = 4.28, N = 8.72 %, Elemental analysis calc. for $C_{40}H_{42}N_6O_{10}Cl_2Cd$: C = 50.55, H = 4.42, N = 8.84%. IR (KBr pellet) cm^{-1}; ν(N-H), 3280s; ν(C=N), 1642s; ν(C=C)+ ν(C=N)py, 1597m; ν(C=C)ph, 1495m; ν(M-N), 521vw; ν(ClO_4^-), 1078br; δ(O-Cl-O), 621s. λ_{max}/nm(ε_{max}/$mol^{-1}cm^{-1}$): 294(3835), 282(5280), 233(8750). $\Lambda_M(CH_3CN)(\Omega^{-1}cm^2mol^{-1})$ = 250.

2(B).2.3. Physical Measurements

The IR spectra of the ligand and all the synthesized complexes were recorded on a Bruker Alpha spectrometer using KBr pellets. The micro analyses (C, H and N) were carried out using a Thermo Finnigan Flash EA 1112 series elemental analyzer. UV-Vis spectra (900 - 190 nm) of the ligand and complexes were recorded on a JASCO V630 in CH_3CN solution (1×10^{-3} M). Equip-Tronics conductivity meter (model no. EQ660 A) was utilized to measure solution conductivity in acetonitrile solution (1×10^{-3} M). Room temperature magnetic susceptibilities of powder samples were measured using Guoy balance.

2(B).2.4 Cell line and culture

Neuroblastoma cancer (SH-SY5Y) cell line was obtained from NCCS, Pune, India and maintained in MEM containing 10% FBS at 37°C in CO_2 incubator.

2(B).2.5 Cytotoxicity (MTT) assay

Neuroblastoma cells were cultured in 96 well plates, after adhesion, cells were exposed to five different concentration of test compound for 24 h for cytotoxicity assay. After treatment cells were washed with PBS (Phosphate buffer saline) and exposed to MTT [3-(4,5-dimethylthiazol-2-yl-)-2,5-diphenyltetrazolium bromide] solution (5mg/ml) for 4h. Formazon [5-(4,5-dimethylthiazole-2-yl)-1,3-diphenylformazon] crystals were dissolved in DMSO solution and OD was measured at 570nm. Cytotoxicity of each concentration was calculated and concentration vs cytotoxicity (inhibition of cell proliferation) graph was prepared. Inhibition concentration 50 (IC50) for each compound was calculated.

2(B).3. X-ray Crystallography

The single crystal X-ray data of compounds **2** and **5** were collected on Oxford X-CALIBUR-S diffractometer equipped with CCD detector. The details of crystallographic data collection and some important features of the structure refinements of the complexes are given in Table 2(B).1. Data were collected with Mo-Kα radiation (λ= 0.71073 Å) at 293 K for all the compounds. The data interpretations were processed with CrysAlisPro, Agilent Technologies, Version 1.171.35.19 [30]. Absorption corrections were applied based on multi-scan method [31]. The structures were solved by direct methods and refined by the full-matrix least-square method based on F^2 technique using SHELXL-97 program package [32]. All calculations were carried out using WinGX system Ver-1.64 crystallographic software [33]. All non-hydrogen atoms were refined anisotropically. ORTEP3 windows program were used for generating for molecular graphics [34].

2(B).4. Results and discussion

2(B).4.1. Syntheses

The mononuclear complexes $[M(L1)_2](ClO_4)_2.2H_2O$ [M = Cu(II), Co(II), Mn(II), NI(II), Zn(II) and Cd(II)] were synthesized with good yield (>65%) upon stirring of 1:2 mole ratio of metal perchlorate salt and tridentate Schiff base L1 in methanol at room temperature [Scheme 2(B). 1]. The ligand L1 is tridentate and has utilized it's all three nitrogen donor atoms for coordination with metal ions in all the mononuclear complexes and this was confirmed by IR data and single crystal X-ray diffraction studies. Molecular composition of the complexes was confirmed by microanalysis, molar conductivity measurements and magnetic study.

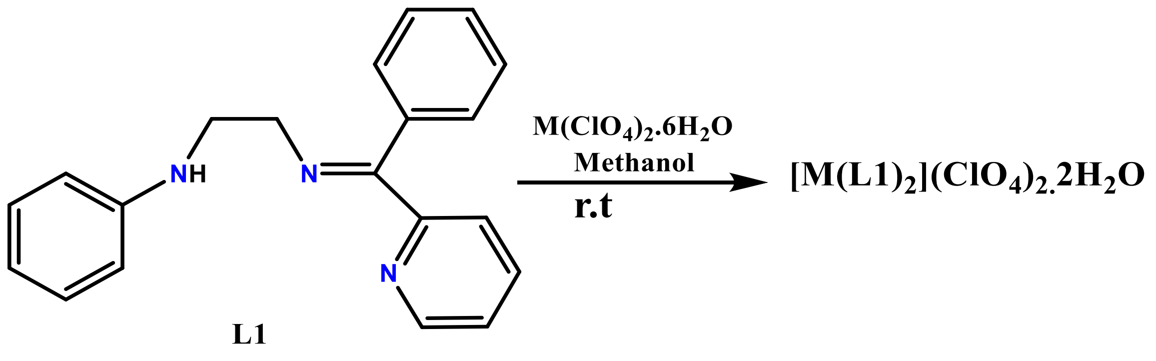

[M = Cu(II), Co(II), Mn(II), NI(II), Zn(II), Cd(II)]

Scheme 2(B).1. Syntheses of the complexes

Table 2(B).1 Crystallographic data for complexes 2 and 5.

	$[Ni(L1)_2](ClO_4)_2.2H_2O$	**$[Zn(L1)_2](ClO_4)_2.2H_2O$**
Empirical formula	$C_{40}H_{42}Cl_2N_6NiO_{10}$	$C_{40}H_{42}Cl_2N_6ZnO_{10}$
Formula weight	896.39	899.05
Temperature(K)	293(2)	293(2)
Crystal system	Monoclinic	Monoclinic
Space group	C2/c	C2/c
a(Å)	33.5919(10)	33.6159(14)
b(Å)	10.0089(3)	9.9488(4)
c(Å)	26.1387(9)	26.4326(14)
α(°)	90	90
β(°)	107.530(4)	108.040(5)
γ(°)	90	90
Volume($Å^3$)	8380.2(5)	8405.5(7)
Z	8	8
ρ_{calc}(g/cm^3)	1.421	1.421
μ(mm^{-1})	0.654	0.775
F(000)	3728.0	3712.0
Crystal size(mm^3)	0.6 × 0.2 × 0.2	0.6 × 0.4× 0.2
Radiation(Å)	Mo Kα (λ = 0.71073	Mo Kα (λ = 0.71073)
2Θ range for data collection (°)	6.12 to 58.02	6.15 to 58.404
Index ranges	-39 ≤ h ≤ 39, -11 ≤ k ≤ 11, -31 ≤ l ≤ 31	-39 ≤ h ≤ 39, -11 ≤ k ≤ 11, -31 ≤ l ≤ 31
Reflections collected	48146	48531
Independent reflections	10152 [R_{int} = 0.04699, R_{sigma} = 0.0432]	10254 [R_{int} = 0.0547, R_{sigma} = 0.0517]
Data/restraints/ Parameters	7355/13/556	10254/0/538
Goodness-of-fit on F^2	1.567	1.504
Final R indexes [I≥2σ (I)]	R_1 =0.0952,wR_2 = 0.0747	R_1 = 0.0983, wR_2 = 0.0748

Final R indexes [all data]	R_1 = 0.2273, wR_2 = 0.2156	R_1 = 0.2305, wR_2 = 0.2123
Largest diff. peak/ hole (eÅ^{-3})	1.31/-0.76	1.20/-0.92
CCDC No.	2144027	2144028

The molar conductivity data of the complexes confirmed 1:2 electrolytes for all the complexes indicating the presence of two perchlorate anions outside the coordination sphere. Structural characterization of the Ni(II) and Zn(II) complexes show both the complexes are mononuclear and have distorted octahedral structure geometry. The spectral and magnetic data indicate all the complexes have octahedral geometry. The compounds are soluble in all common organic solvents like acetonitrile, alcohol, acetone, dichloromethane etc.

2(B).4.2. Spectral Data

2(B).4.2.1. ESI-Mass spectral data

Mass spectrum of the complexes were taken ESI method and the mass spectrum of all the complexes showed the molecular ion peaks with m/z = 301 correspond to molecular ion of Schiff base ligand $[C_{20}H_{19}N_3]^+$ ion. The spectrum of Cu(II) complex showed a molecular ion peak at m/z = 663.71 and the actual molecular mass of [Cu(II)+2L1] is 665.5 indicating metal

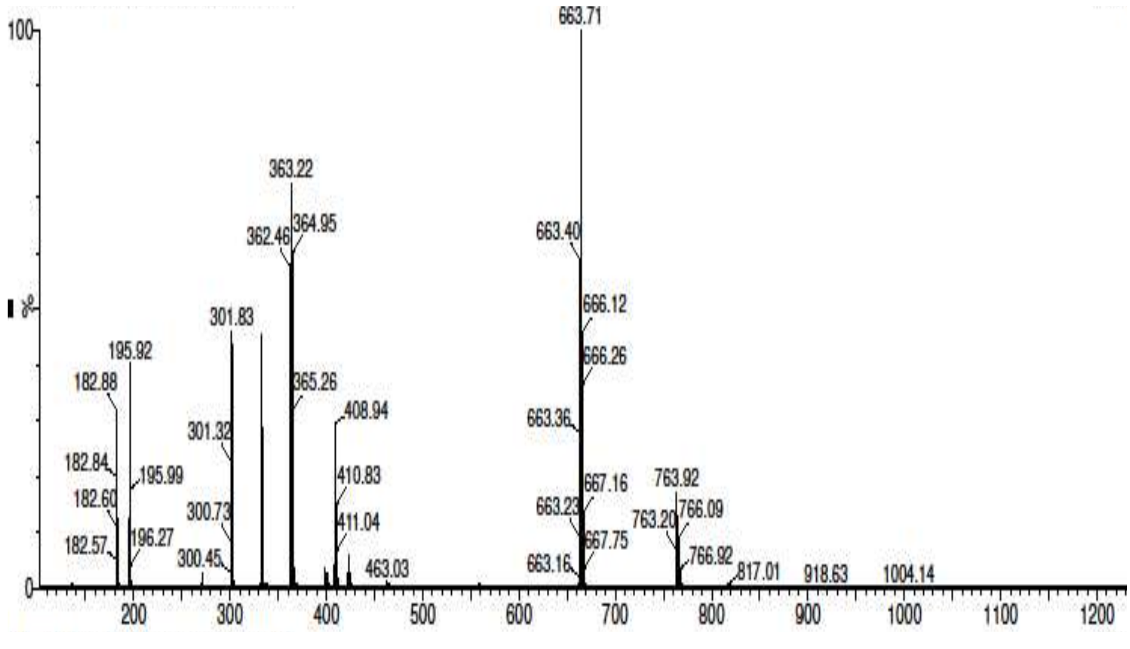

m/z

Figure.2(B).1. ESI-Mass spectrum of $[Cu(L1)_2](ClO_4)_2.2H_2O$

and ligand ratio is 1:2 in the complex. Similarly, the mass spectrum of Co(II), Mn(II) and Zn(II) complexes showed molecular ions at m/z 659.88, 656.98 and 665.25, respectively and the calculate mass of the complexes are 660.93[Co(II)+2L1]$^+$, 657.93 [Mn(II)+2L1]$^+$and 666.25 [Zn(II)+2L1]$^+$ respectively. The mass spectral data of the complexes show the expected molecular ion components and confirm the proposed structures.

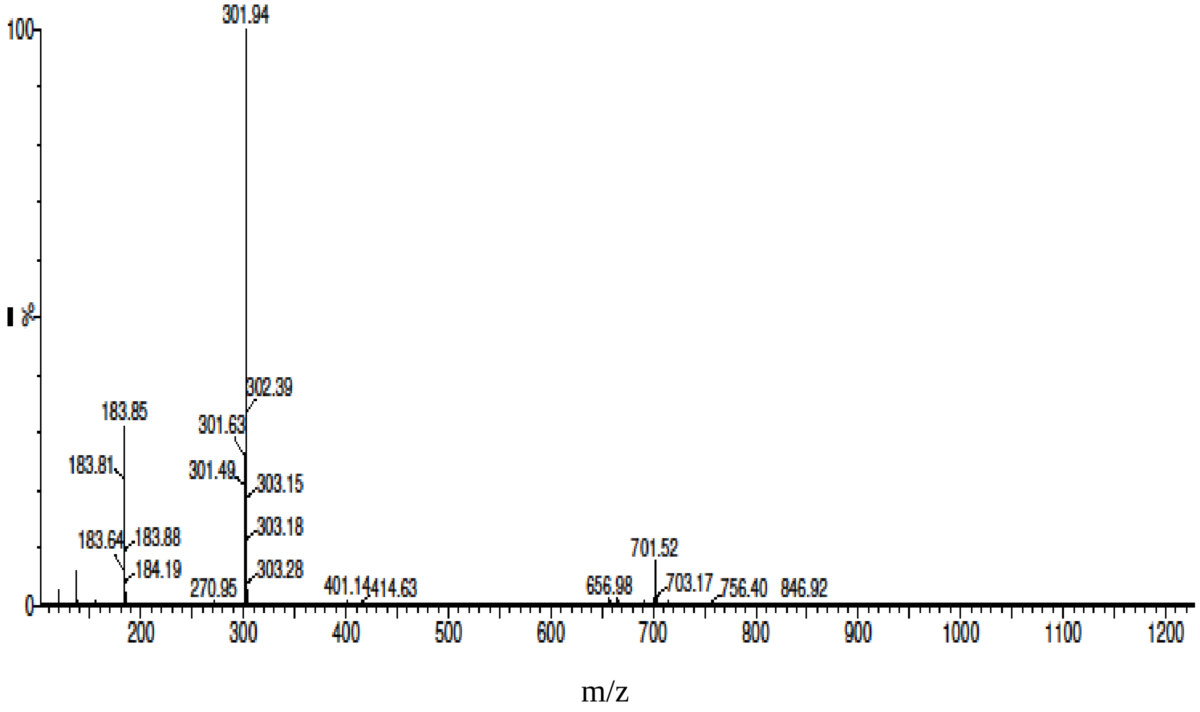

Figure.2(B).2. ESI-Mass spectrum of $[Mn(L1)_2](ClO_4)_2.2H_2O$

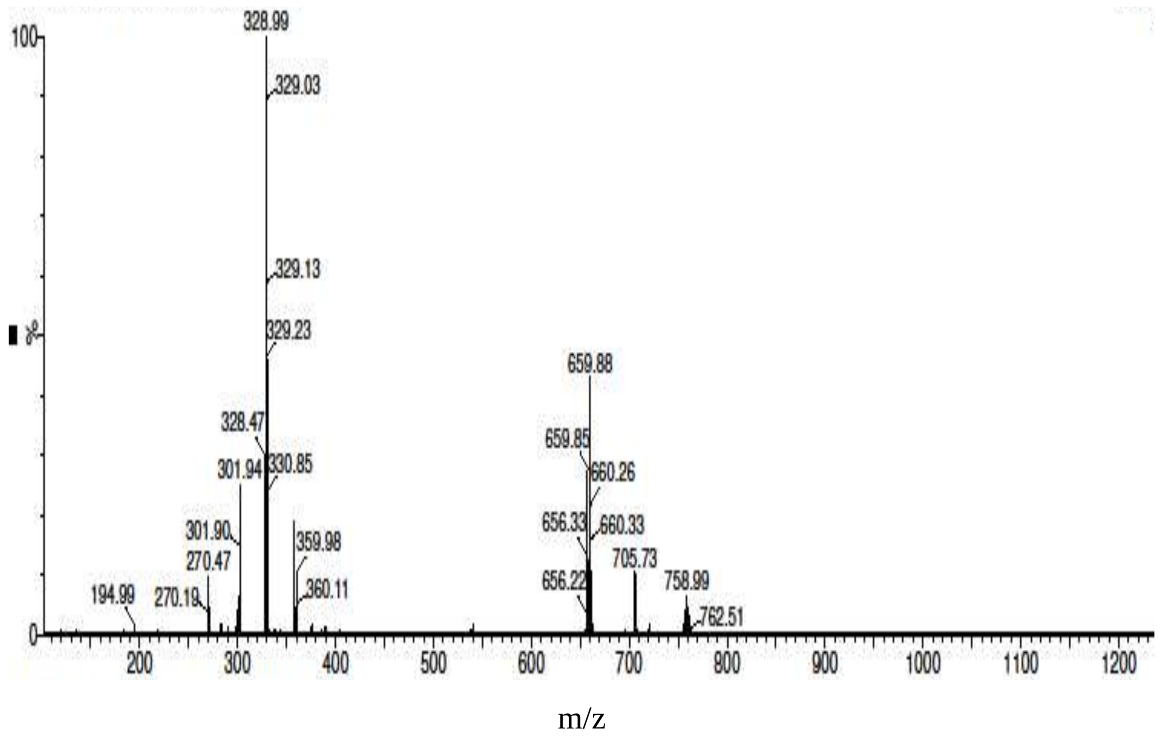

Figure.2(B).3. ESI-Mass spectrum of $[Co(L1)_2](ClO_4)_2.2H_2O$

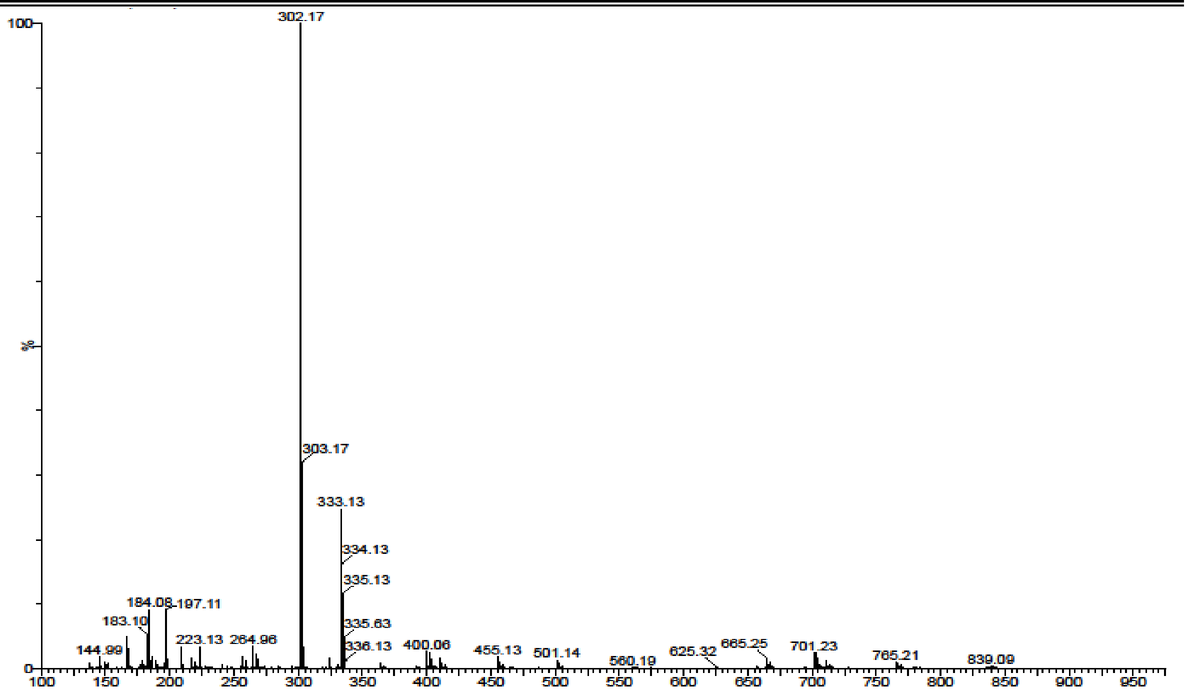

Figure.2(B).4. ESI-Mass spectrum of $[Zn(L1)_2](ClO_4)_2.2H_2O$

2(B).4.2.2. IR spectral data

The IR spectra of the complexes exhibited several strong bands and were assigned in comparison to the spectra of the Schiff base ligand L1. In all the complexes, one sharp band exhibited at ~3244 cm^{-1} due to ν(NH) and another strong absorption band exhibited at ~1639 cm^{-1} due to ν(C=N) group. These two absorption bands are also present in the ligand but shifted to lower wave numbers which may be attributed to the coordination of the ligand with the metal centres. All the complexes show two bands- one broad band in the range of 1070-1100 cm^{-1} and another δ(O-Cl-O) at 621 cm^{-1} indicating the presence of ClO_4^- outside the coordination sphere [35].

2(B).4.2.3. Electronic spectral data

The UV-Vis spectra of the complexes were recorded in the range of 190-1000 nm in CH_3CN (conc.10^{-3} M). For all complexes, the high intensity bands appeared at less than 400 nm correspond to ligand n- π* / π - π* charge transfer transitions. In the visible region, one broad absorption band was observed for copper (II) complex at 650 nm and this is due to d-d transition. This type of spectra is typical for Cu(II) complex with octahedral geometry[36].

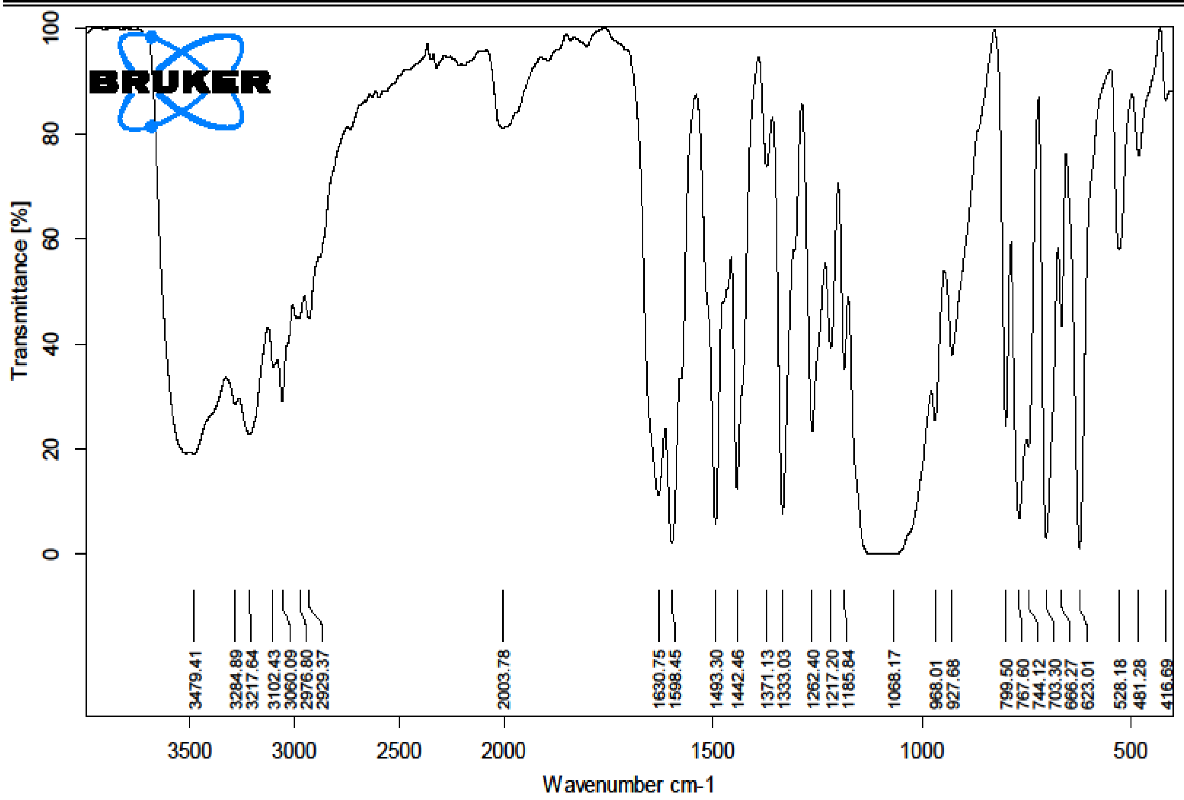

Figure. 2(B).5. IR spectrum of $[Cu(L1)_2](ClO_4)_2.2H_2O$

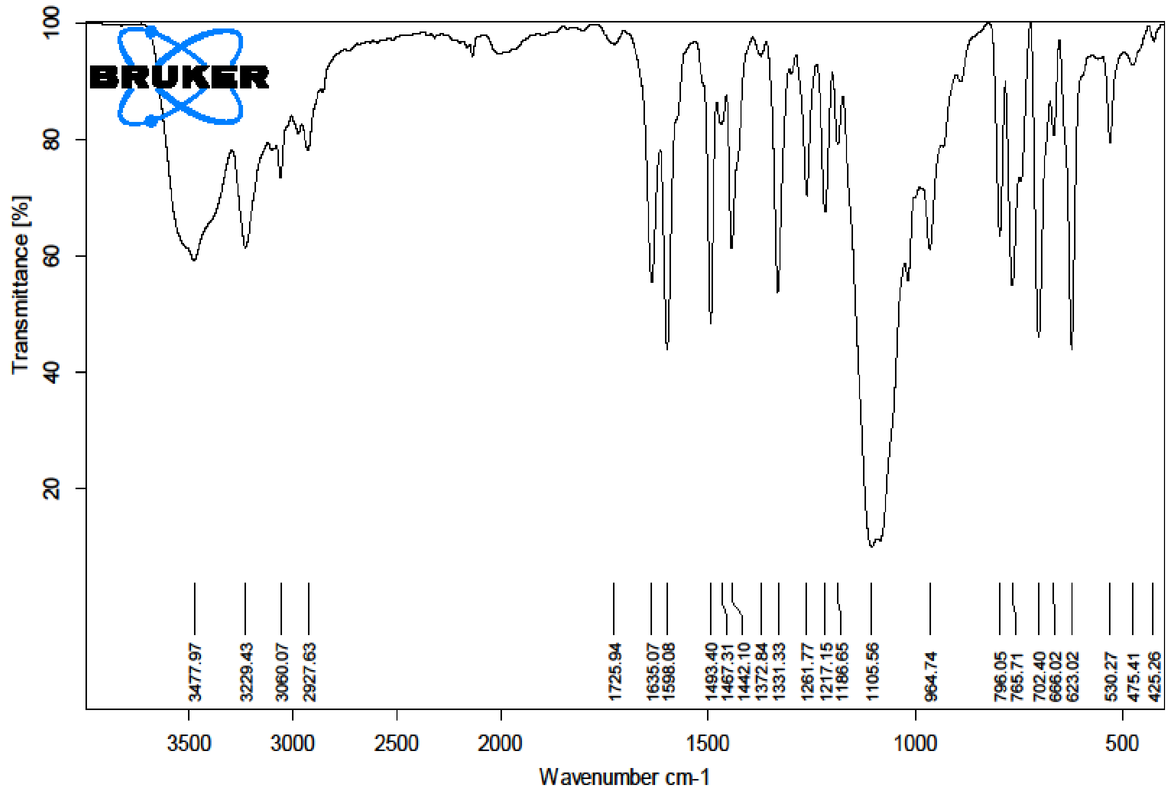

Figure.2(B).6. IR spectrum of $[Ni(L1)_2](ClO_4)_2.2H_2O$

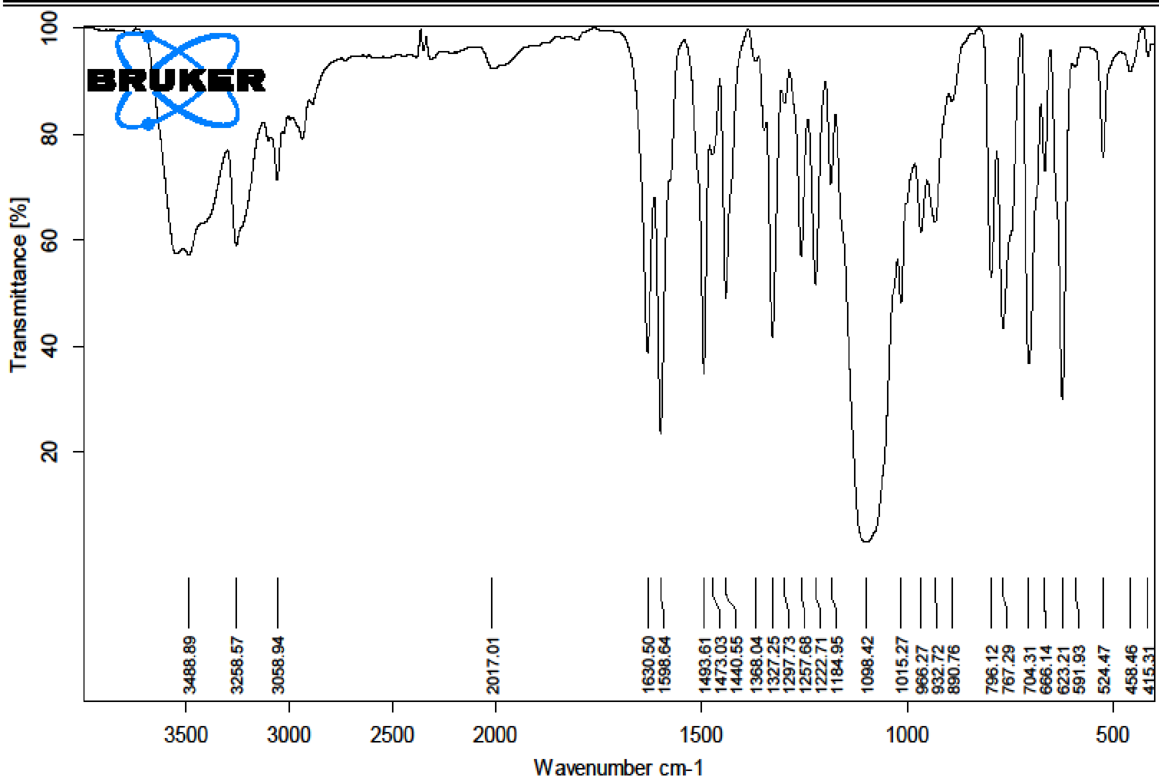

Figure.2(B).7. IR spectrum of $[Mn(L1)_2](ClO_4)_2.2H_2O$

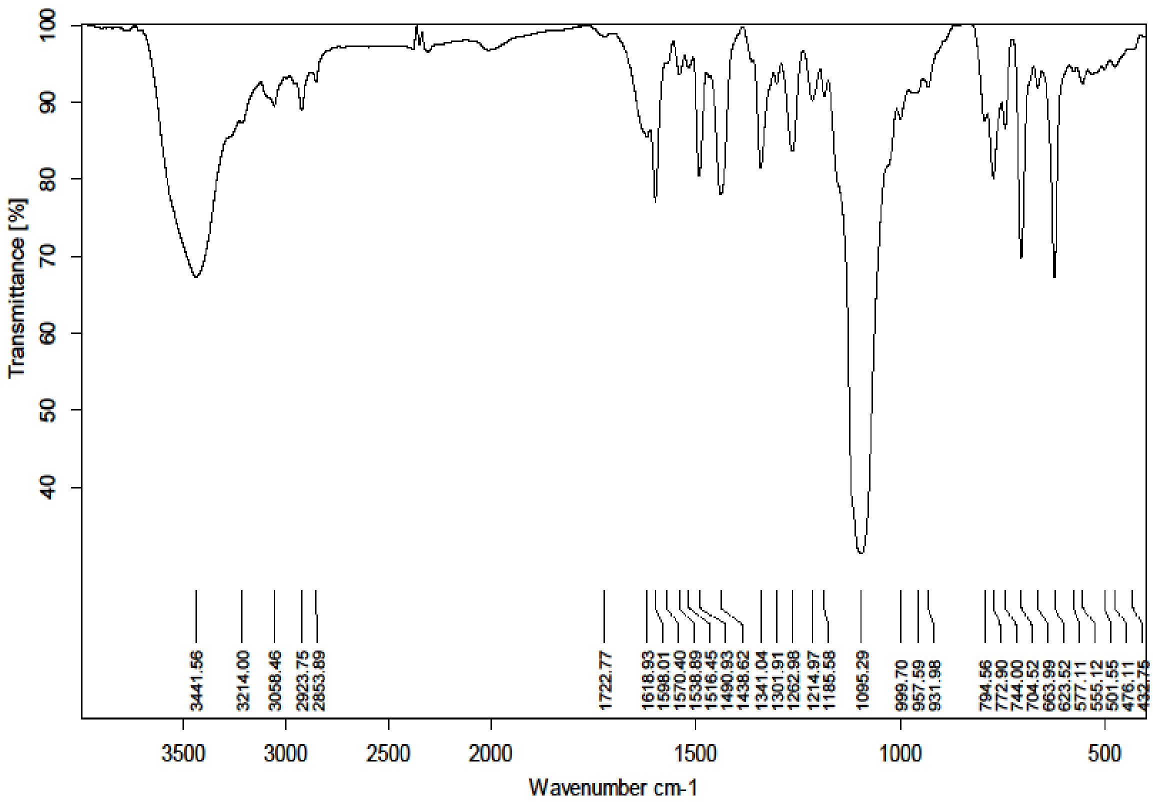

Figure.2(B).8. IR spectrum of $[Co(L1)_2](ClO_4)_2.2H_2O$

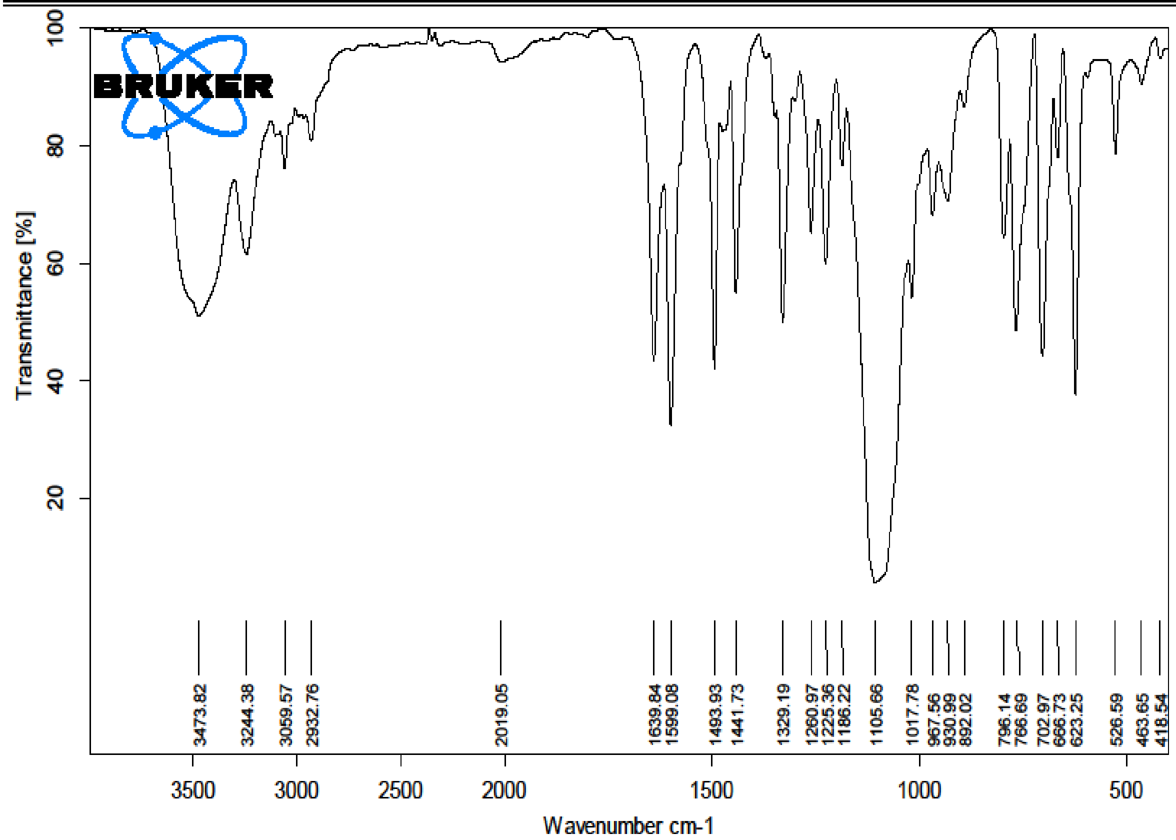

Figure.2(B).9. IR spectrum of $[Zn(L1)_2](ClO_4)_2.2H_2O$

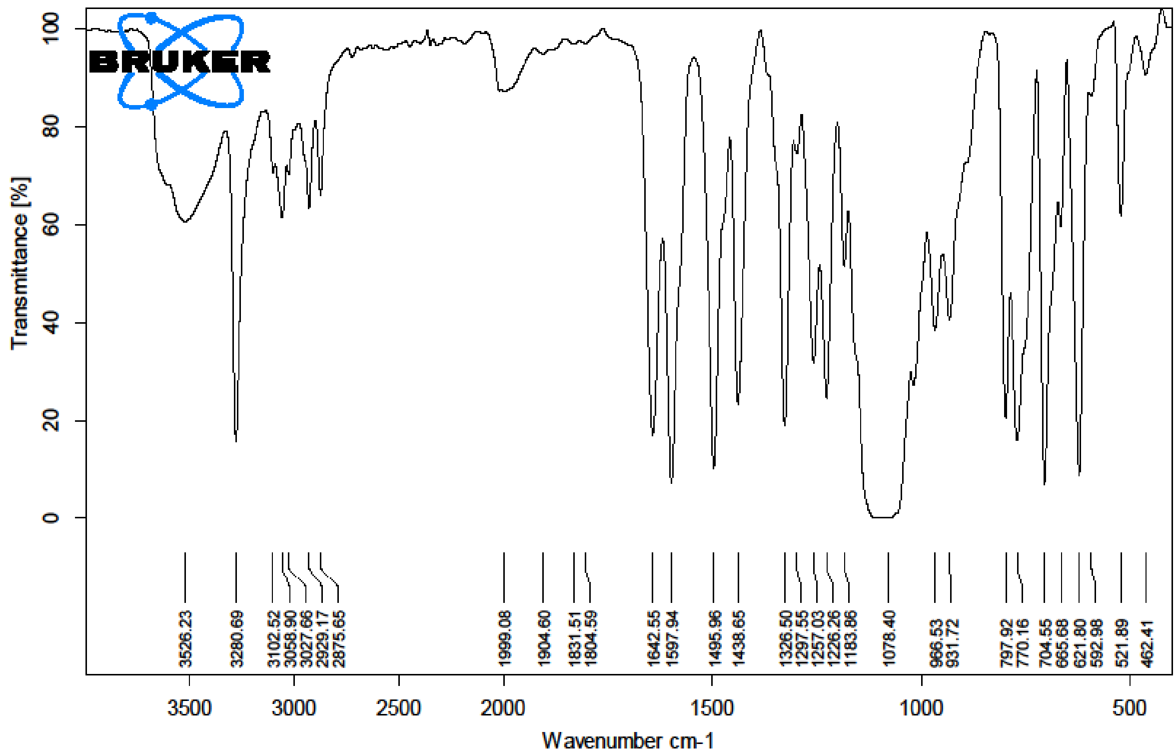

Figure.2(B)10. IR spectrum of $[Cd(L1)_2](ClO_4)_2.2H_2O$

Similarly, nickel(II) complex exhibited two absorption bands at 568 and 469 nm and Co (II) complex exhibited two absorption bands at 841 and 521 nm and these are due to d-d transition or ligand field transitions. This type of transitions is generally observed for high spin cobalt (II) complexes [37].

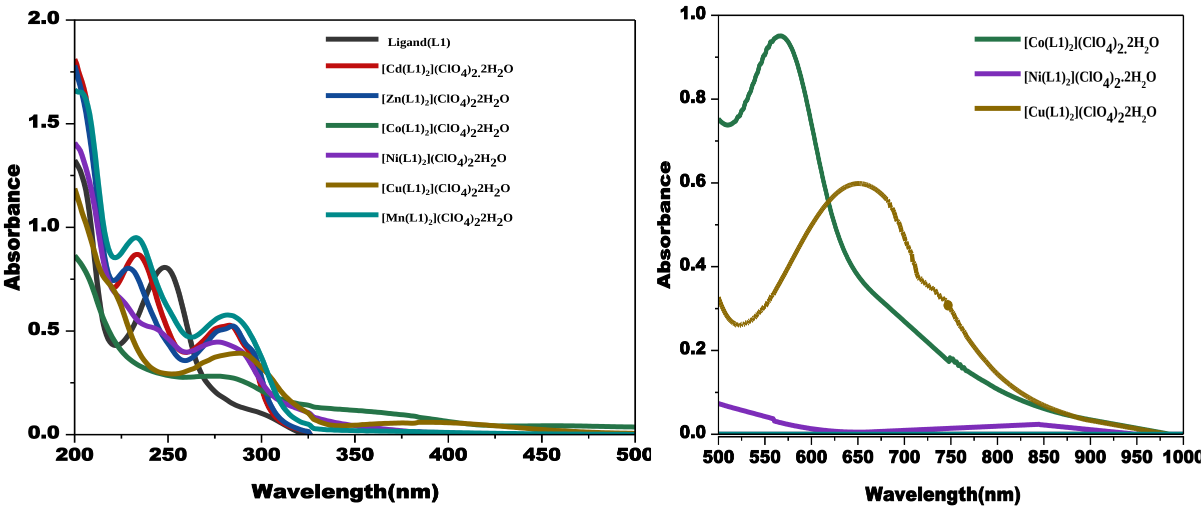

Figure. 2(B).11. Electronic spectra of the ligand(L1) and complexes in CH_3CN (10^{-3} M).

2(B).4.2.4. Magnetic studies

The magnetic susceptibility measurement of the powder samples shows that the effective magnetic moment (μ_{eff}) of the complexes are 1.82, 2.75, 3.87 and 5.82 BM for Cu(II), Ni(II), Co(II) and Mn(II) complexes, respectively indicating the presence of one unpaired electron in Cu(II), two unpaired electrons in Ni(II), three electron in Co(II) and five unpaired electrons in Mn(II) complexes.

2(B).4.2.5. EPR spectra

The X-band EPR spectrum of copper(II) complex was recorded in DMSO solution at liquid nitrogen temperature (77 K) and exhibited a typical four line splitting pattern with well resolved hyperfine peaks. This is due to interaction of the unpaired electron with the nuclear spin of the copper nucleus (^{63,65}Cu: I = 3/2). The g_{II} and $g_{\perp}$ values of the complex are 2.226 and 2.077, respectively. The observed feature $g_{II} > g_{\perp} > 2$ is diagnostic of a pseudotetragonal site for copper(II) and the ground states of Cu(II) is predominantly $dx^2 - y^2$.

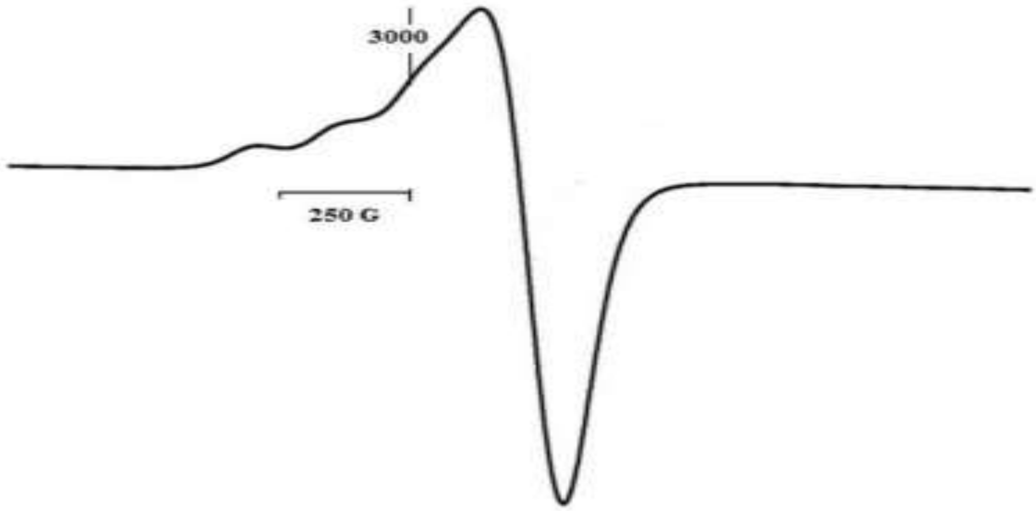

Figure 2(B).12. X-Band EPR spectrum of Cu(II) complex in DMSO at 77 K

2(B).4.3. Descriptions of Crystal Structures

2(B).4.3.1. Crystal structure of the $[Ni(L1)_2](ClO_4)_2.2H_2O$

The ORTEP diagram of the complex with atom-labelling scheme is shown in Fig. 2(B).13 and selected bond lengths and angles are given in Table 2(B).3. The molecule crystallizes in monoclinic crystal system with space group C2/c. The structure determination confirmed that the complex is ionic and each molecule has two perchlorate anions and two water molecules outside the coordination sphere. In the structure, nickel(II) has six coordination and is surrounded by six nitrogen atoms from two tridentate ligands. The equatorial positions of the octahedron are occupied by four nitrogen atoms N1, N2, N3 and N5 and the axial positions are occupied by two nitrogen atoms N4 and N6. The bond distance Ni–N1(2.222 Å) is longer than the other three bond lengths Ni–N2(2.005), Ni–N3(2.096 Å) and Ni–N5(2.010 Å) in the equatorial plane. The bond distances in the axial planes Ni–N4(2.227 Å) and Ni–N6(2.116 Å) are not equal and the axial bond angle N4–Ni1–N6 (157.69^0) is not linear. The bond angles of N5-Ni-N2 (175.68) and N3-Ni-N1 (157.69) are not linear. The geometry around the nickel (II) centre is distorted octahedral which can be described from unequal bond angles and bond lengths.

In the molecule, oxygen atom O9 of H_2O molecule has short intermolecular interaction with H1 of NH1 and H4 of H4N4. Similarly, H51 of H51O9 has short interaction with one oxygen atom O1 of ClO_4^- ion and another hydrogen atom i.e. H50 of H51O9 has short interaction O10 of another water molecule. One H atom from another water molecule i.e. H53 of H53O10 has short interaction with one oxygen atom O8 of ClO_4^- ion.

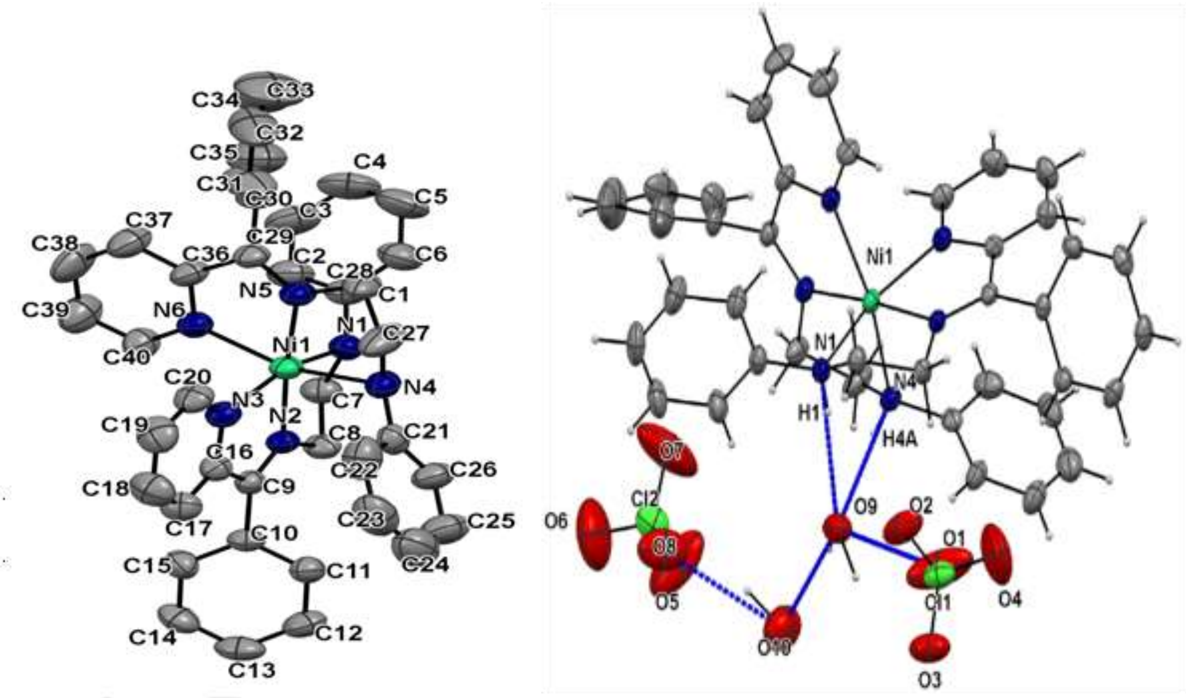

Figure.2(B).13(a). ORTEP diagram of the cationic part of the complex $[Ni(L1)_2](ClO_4)_2.2H_2O$ with atom numbering scheme (50% probability factor for the thermal ellipsoids). H-atom and H_2O and perchlorate molecules are omitted for clarity. (**b).** Intermolecular interaction of complex **2**

Table 2(B).2 Intermolecular interaction of the Ni(II) Complex

Compounds/parameters	D–H(Å)	H—A(Å)	D——A(Å)	<(DHA
$[Ni(L1)_2](ClO_4)_2.2H_2O$ (2)				
N1-H1-O9	0.798	2.260	3.054	174.24
N4-H4A-O9	0.800	2.261	3.053	170.29
O9-H51-O1	0.950	2.550	2.978	107.34
O9-H50-O10	0.994	1.897	2.681	133.63
O10-H53-O8	1.051	2.088	3.016	145.77

Table 2(A). 3 Selected bond lengths (A°) and Bond angles (°) of the complexes 2 and 5

Bond lengths (A°)				**Bond angles (°)**			
[Ni(L1)$_2$](ClO$_4$)$_2$.2H$_2$O		**[Zn(L1)$_2$](ClO$_4$)$_2$.2H$_2$O**		**[Ni(L1)$_2$](ClO$_4$)$_2$.2H$_2$O**		**[Zn(L1)$_2$](ClO$_4$)$_2$.2H$_2$O**	
Ni1-N2	2.005(3)	Zn1 - N2	2.066(4)	N2-Ni1-N5	175.69(14)	N2 -Zn1-N5	172.11(14)
Ni1-N5	2.010(3)	Zn1 - N5	2.066(3)	N2-Ni1-N3	77.67(13)	N2-Zn1-N3	76.85(15)
Ni1-N3	2.096(4)	Zn1 - N3	2.160(4)	N5-Ni1-N3	104.65(14)	N5-Zn1-N3	110.36(14)
Ni1-N6	2.115(3)	Zn1 - N6	2.159(4)	N2-Ni1-N6	105.59(13)	N2 -Zn1-N6	107.22(15)
Ni1-N1	2.222(4)	Zn1 - N4	2.317(4)	N5-Ni1-N6	78.20(14)	N5 -Zn1-N6	76.26(14)
		Zn1- N1	2.367(4)	N3-Ni1-N6	89.48(14)	N3-Zn1-N6	92.38(14)
				N2-Ni1-N1	80.63(13)	N2-Zn1-N4	98.23(16)
				N5-Ni1-N1	97.24(15)	N5-Zn1-N4	78.39(14)
				N3-Ni1-N1	158.02(13	N3-Zn1-N4	94.14(15)
				N6-Ni1-N1	93.05(14)	N6-Zn1-N4	154.54(14)
				N2-Ni1-N4	96.41(13)	N2-Zn1-N1	77.22(14)
				N5-Ni1-N4	79.96(14)	N5-Zn1-N1	95.80(14)

2(B).4.3.2. Description of structure of $[Zn(L1)_2](ClO_4)_2.2H_2O$

The ORTEP diagram of the complex with atom numbering scheme is shown in Fig. 2(B).14. The molecule crystallizes in the monoclinic crystal system with space group *C2/c* . The structure shows zinc centre has octahedral geometry and two tridentate ligands are coordinated to the zinc centre. Two perchlorate anions and two water molecules are outside the coordination sphere. The bond distances in the equatorial plane show the Zn-N1(2.366Å) is much longer than other three equatorial Zn-N2 (2.006Å), Zn-N3(2.160Å) and Zn-N5(2.006Å) bond distances. The bond angle of N1-Zn-N3 (153.67) is much deviate compare to the bond angle N2-Zn-N5 (172.11^0). The axial bond distance of Zn-N4(2.317Å) is longer than Zn-N6(2.159 Å) and the axial bond angle N4–Ni–N6 is 154.53^0 is not linear. The geometry around the zinc (II) centre is distorted octahedral which are due to unequal bond angles and bond lengths.

In the molecule, hydrogen atom H40 of C40H40 has short interaction with one oxygen atom O8 of ClO_4^- ion and another oxygen atom O6 of ClO_4^- ion has intermolecular H-bonding interaction with H7B of H7BC7.

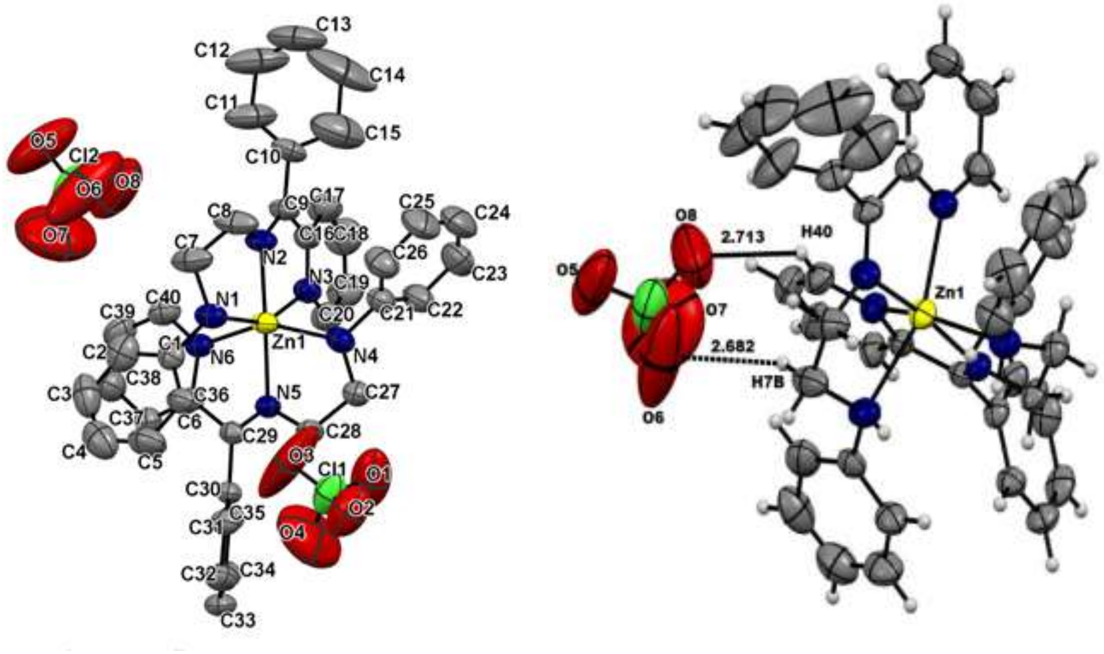

(a) **(b)**

Figure.2(B).14(a). ORTEP diagram of the complex $[Zn(L1)_2](ClO_4)_2.2H_2O$ with atom numbering scheme (50% probability factor for the thermal ellipsoids) H-atom and H_2O molecule are omitted for clarity. **(b).** Intermolecular H-bonding interaction in complex 5.

Table 2(B).4 Intermolecular hydrogen bonds of the Zn(II) Complex

Compounds/parameters	D–H(Å)	H—A(Å)	D——A(Å)	<(DHA
$[Zn(L1)_2](ClO_4)_2.2H_2O$				
C40-H40-O8	0.930	2.713	3.442	135.88
C7-H7B-O6	0.970	2.682	3.344	125.86

2(B).4.4. Cytotoxicity assay

MTT assay was carried out to check for the cytotoxicity potential of the metal complexes. These metal complexes were then compared with their respective metal salts and ligand to study the alteration in their cytotoxicity behaviour. The IC50 values (concentration required for 50% inhibition of cell growth) are listed in Table 2(B).5. From the results, compared to the ligand, complexes have higher activities due to the presence of metal moieties and chelation in the compounds [38].

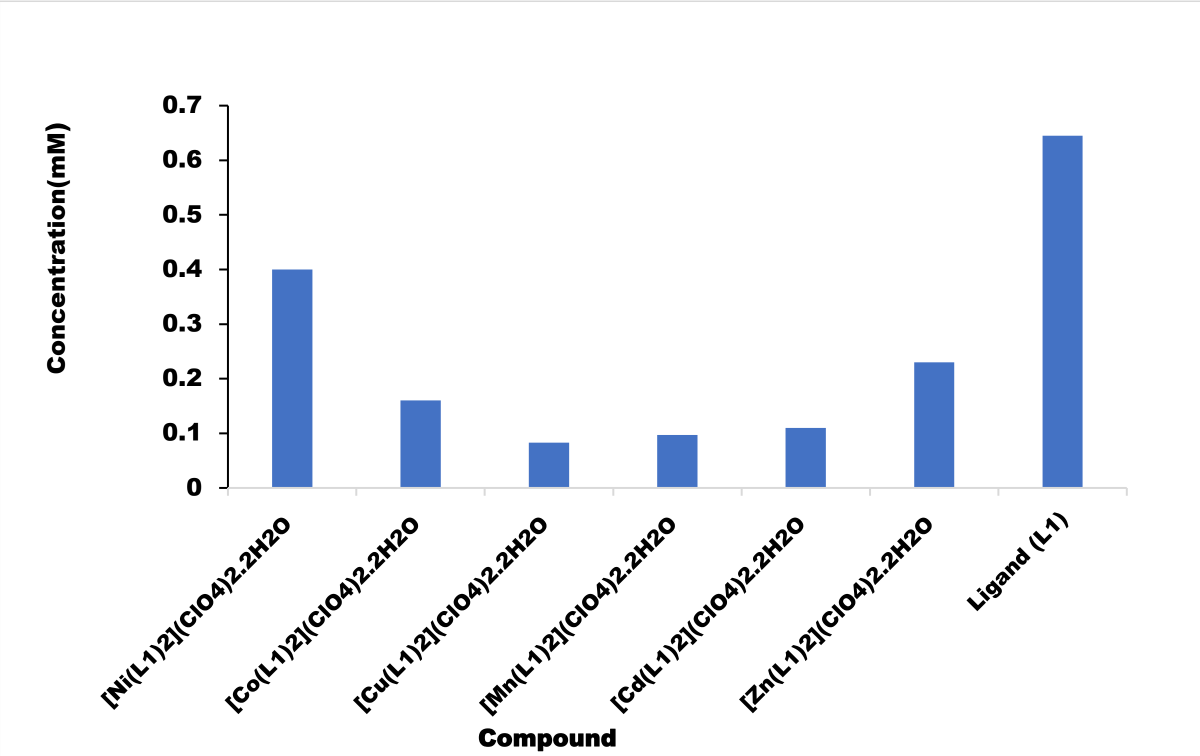

Figure.2(B).15. Cytotoxicity activity of the ligand (L1) and it's M(II) complexes were tested against neuroblastoma cancer cell line (SH-SY5Y)

The activity of the synthesized compounds **(1-6)** and their respective ligands show that all complexes have better activity than respective ligands against SH-SY5Y cancer cell lines. It is clearly observed that complexation with metals has a synergetic effect on the biological activity of these compounds and the biological activity depends upon the type of metal ion. Copper and manganese complexes had quite contrasting effect compared to their salts and ligand. This confirms the conclusion that the cytotoxic activities of Schiff base can be enhanced by coordinating the ligand to Cu(II) and Mn(II) cations [39-41]. Copper(II) and manganese(II) showed potent cytotoxicity activity and had IC50 value are 0.083 are 0.097 mM, respectively, whereas all the other complexes exhibit moderate cytotoxic effect.

Table 2(B).5 IC50 Value of the complexes.

Compound	IC50 (mM)
$[Cu(L1)_2](ClO_4)_2.2H_2O$	0.083
$[Ni(L1)_2](ClO_4)_2.2H_2O$	0.40
$[Mn(L1)_2](ClO_4)_2.2H_2O$	0.097
$[Co(L1)_2](ClO_4)_2.2H_2O$	0.16
$[Zn(L1)_2](ClO_4)_2.2H_2O$	0.23
$[Cd(L1)_2](ClO_4)_2.2H_2O$	0.11
Ligand (L1)	0.645

2(B).5. Conclusion

The tridentate N_3-coordinate ligand N′-Phenyl-N″(phenyl(pyridin-2-yl)methylene)-ethane-1,2-diamine(L1) has been used in the synthesis of a series of six mononuclear octahedral complexes $[M(L1)_2](ClO_4)_2.2H_2O$ [M = Cu(II), Co(II), Mn(II), Ni(II), Zn(II) and Cd(II)] and the complexes were characterized by spectroscopic techniques and single crystal X-ray diffraction studies. Structural data shows all have distorted octahedral geometry and cytotoxic activities of the complexes showed they have dose depended cytotoxic activity.

2(B).6. References

1. H. Schiff, Ann. Chem. Suppl. 3 (1864) 343.
2. M. Pervaiz, S. Sadiq, A. Sadiq, U. Younas, A. Ashraf, Z. Saeed, M. Zuber, A. Adnan. Coord. Chem. Rev. 447 (2021) 214128.
3. M. Abu-Dief, I. M. A. Mohamed. Beni-Suef University J. Basic and Appl. Sci.4 (2015) 119.
4. D. Majumdar, J. E. Philip, S. Das, B. Kundu, R. Saini, G. Chandan, K. Bankura, D. Mishra. J. Mol. Struct. 1225 (2021) 129189.
5. K. Gupta, A. K. Sutar. Coord. Chem. Rev. 252 (2008) 1420.
6. W. Al Zoubi, Y.G. Ko. Organomet. Chem. 31 (2017) e3574.
7. N. Mohan, S. S. Sreejith, R. George, P.V. Mohanan, M. R. Prathapachandra Kurup. J. Mol. Struct. 1229 (2021) 129779.
8. N. Mohan, S.S. Sreejith, P.S. Begum, M. R. P. Kurup. New J. Chem. 42 (2018) 13114.
9. T. Shiga, K. Maruyama, G.N. Newton, R. Inglis, E.K. Brechin, H. Oshio. Inorg. Chem. 53 (2014) 4272.
10. Pogány, J. Moncol, J. Pavlik, M. Mazúr, I. Salitros. ChemPlusChem 84 (2019) 358.
11. R. H. Taha, Z. A. El-Shafiey, A. A. Salman, E. M. El-Fakharany, M. M. Mansour. J. Mol. Struct. 1181 (2019) 536.
12. S. Dolai, K. Das, A. Bhunia, V. Bertolasi, S.C. Manna. Appl. Organomet. Chem. 32 (2018) 4506.
13. B. Kumari, S. Kundu, K. Ghosh, M. Banerjee, S. K. Pradhan, Sk. M. Islam, Paula Brandão, V. Félix, D. Das. Dalton Trans. (2018).
14. Z. Guo, R. Xing, S. Liu, Z. Zhong, X. Ji, L. Wang, et al. Carbohydrate Res. 342 (2007) 1329.
15. (a) D. N. Dhar, C.L. Taploo. J. Sci. Ind. Res. 41 (1982) 501.
    (b) P. Przybylski, A. Huczynski, K. Pyta, B. Brzezinski, F. Bartl. Curr. Org. Chem. 13 (2009) 124.
16. S. Ambika, Y. Manojkumar, S. Arunachalam, B. Gowdhami, K. K. M. Sundaram, R. V. Solomon, P. Venuvanalingam, M. A. Akbarsha, M. Sundararaman. Scientific reports 9 (2019) 2721.

17. M. Sakthi, A. Ramu. J. Mol. Struct. 1149 (2017) 727.
18. M. A. Malik, O. A. Dar, P. Gull, M. Y. Wani, A. A. Hashmi. Med. Chem. Comm. 9 (2018) 409.
19. X. Liu, J. R. Hamon. Coord. Chem. Rev. 389 (2019) 94.
20. H. Kargar, V. Torabi, A. Akbari, R. Behjatmanesh-Ardakani, A. Sahraei, M. N. Tahir. Struct. Chem. 30 (2019) 2289.
21. K. Yasser Abdel-Monem, A. Saeyda Abouel-Enein, M. Safa El-Seady. J. Mol. Struct. 1152 (2018) 115.
22. K. Ghosh, K. Harms, A. Bauzá, A. Frontera, S. Chattopadhyay. Dalton Trans. 47 (2018) 331.
23. T. Basak, K. Ghosh, C. J. Gómez García, S Chattopadhyay. Polyhedron 146 (2018) 42.
24. S. Thakur, S. Banerjee, S. Das, S. Chattopadhyay. New J. Chem. 43 (2019) 18747.
25. J. Pérez-Pérez, J.G. Alvarado-Rodríguez, N. Andrade-López, J.C. Borbolla, D. Martínez-Otero, J.M. Vásquez-Pérez, Inorg. Chem. Commun. 70 (2016) 75.
26. D. Majumdar, J. Elizabeth Philip, S. Das, B. Kundue, R. Saini, G. Chandan, K. Bankuraa, D. Mishra. J. Mol. Struct. 1225 (2020) 129189.
27. H. Kargar, A. Adabi Ardakani, M. Nawaz Tahir, M. Ashfaq, K. Shahzad Munawar. J. Mol. Struct. 1233 (2021) 130112.
28. L. Mei, S. Huang, C. Ye, Y. Xie. Spectrochimica Acta Part A: Mol. Biomol. Spect. 150 (2015) 290.
29. S. J. Munshi, J. K. Saini, S. Ingle, S. B. Kumar. J. Coord. Chem. 74 (2021) 2004.
30. Agilent, CrysAlis PRO. Agilent Technologies UK Ltd, Yarnton, England (2011).
31. G. M. Sheldrick. SAINT, 5.1st edn. Siemens Industrial Automation Inc., Madison, WI (1995).
32. G. M. Sheldrick. SHELXL 97 Program for Crystal Structure Refinement, University of Gottingen, Gottingen
33. L. J. Farrugia. J. Appl Cryst. 32 (1999) 837.
34. L. J. Farrugia. J. Appl. Cryst. 30 (1997) 565.

35. Nakamoto K., Infrared and Raman Spectra of Inorganic and Coordination Compounds, Part B: Applications in Coordination, Organometallic and Bioinorganic Chemistry, fifth ed., Wiley, New York (1997) 116.
36. G. Ahumada, T. Roisnel, S. Kahlal, D. Carrillo, R. Cordova, J. Y Saillard, J.R. Hamon, C. Manzurthis. Inorg. Chim. Acta 470 (2018) 221.
37. G. Achilleas, K. Spyridoula, P. R. Catherine. Inorg. Chem. Commun. 3 (2000) 251.
38. R. Fekri, M. Salehi, A. Asadi, M. Kubick. Inorg. Chim. Acta (2018).
39. N. Farrell. Coord. Chem. Rev. 232 (2002) 1.
40. B. Seth, S. Haldar, P. Chakraborty, P. Saha, S. Basu. J. Photochem. Photobio. B. Biol. 162 (2016) 463.
41. S. Osman, H. Mousa, H. Yosef, T. Hafez, A. El-sawy, M. Abdallah, A. Hassan J. Serb. Chem. Soc. 79 (2014) 953.